THE UNIVERSITY OF CHICAGO

THE ROLES OF COPROPHAGIA AND AMPICILLIN-RESISTANT COMMENSAL BACTERIA IN GUT MICROBIOTA-MEDIATED COLONIZATION RESISTANCE TO VANCOMYCIN-RESISTANT ENTEROCOCCUS

A DISSERTATION SUBMITTED TO THE FACULTY OF THE DIVISION OF THE BIOLOGICAL SCIENCES AND THE PRITZKER SCHOOL OF MEDICINE IN CANDIDACY FOR THE DEGREE OF DOCTOR OF PHILOSOPHY

COMMITTEE ON IMMUNOLOGY

BY

ROSEMARY LYNETTE POPE

CHICAGO, ILLINOIS

JUNE 2025

Copyright 2025 by Rosemary Lynette Pope

All Rights Reserved

TABLE OF CONTENTS

LIST OF FIGURES	v
LIST OF TABLES.	vii
ACKNOWLEDGEMENTS	.viii
ABSTRACT	X
1. INTRODUCTION	
1.1 Vancomycin-resistant Enterococcus faecium (VRE)	1
1.2 Colonization resistance to VRE	
1.3 Influence of the gut microbiota and metabolites on the intestinal immune system	3
1.4 Antibiotic-resistance in commensal bacteria	6
1.5 Summary of project rationale	7
2. MATERIALS AND METHODS	8
2.1 Experimental model and subject details	8
2.1.1 Mouse subjects	
2.1.2 Tail cups and mock cups	8
2.1.3 Ampicillin Treatment	
2.1.4 Bacterial isolates from human donors	
2.1.5 Infection Models	9
2.1.6 Fecal microbiota transplant (FMT) into germ-free (GF) mice	10
2.2 Experimental method details	10
2.2.1 16S rRNA gene sequencing and analysis	10
2.2.2 16S rRNA gene qPCR	
2.2.3 Quantitative and qualitative metabolomics	
2.2.4 Reg3g quantification from the ileum	
2.2.5 Quantification of pathogen burden	14
2.2.6 Microscopy imaging and analysis	14
2.2.7 Shallow shotgun sequencing and analysis	.15
2.2.8 Ampicillin-resistance testing of the fecal microbiota	16
2.2.9 Isolation of bacteria from H47 fecal microbiota	
2.2.10 Isolate susceptibility to ampicillin and beta-lactamase detection assay	17
2.2.11 Whole-genome shotgun sequencing and assembly	17
2.2.12 Identification of beta-lactamase genes in bacterial isolate genomes	.18
2.2.13 Analysis of beta-lactamase genes in metagenomic reads	
2.2.14 Assessment of genes in other bacterial genomes	
2.2.15 <i>In vitro</i> VRE competition/suppression assay with isolates	
2.3 Quantification and statistical analysis	19
3. PREVENTION OF COPROPHAGIA IN MICE ENABLES FULL RESOLUTION OF TH	ΗE
BIOGEOGRAPHIC DISTRIBUTION OF THE INTESTINAL MICROBIOTA AT	
HOMEOSTASIS AND DURING INFECTION WITH VRE	21
3.1 Introduction	21

3.2 Construction of functional tail cup devices to prevent coprophagia in mice	23
3.3 Prevention of coprophagia leads to loss of anaerobic bacteria in upper GI tra	
3.4 Impact of coprophagia on the microbiome metabolites	
3.5 Coprophagia increases activation of the intestinal immune system	
3.6 Coprophagia prolongs VRE infection, but is not necessary for colonization	
antibiotic-treated SI.	
3.7 Prevention of coprophagia enables faster clearance of VRE in the SI	
3.8 <i>E. faecium</i> colonizes the SI epithelium in small clusters	
3.9 Summary of results.	
3.5 Summary of results	
4. COMMENSAL BACTERIA SHIELD THE GUT MICROBIOTA FROM AMPICI	I I IN.
INDUCED DYSBIOSIS AND PRESERVE COLONIZATION RESISTANCE AGAIN	
ANTIBIOTIC-RESISTANT PATHOBIONTS	
4.1 Introduction	
4.2 One out of the seven different mouse microbiota tested was resistant to amp	
induced dysbiosis	
4.3 Ampicillin-resistant microbiota retain production of most bile acid and shor	
fatty acid metabolite compounds after perturbation with ampicillin	
4.4 Ampicillin-resistant bacteria isolated from the H47 microbiome	
4.6 Ampicillin-resistant microbiomes retain their colonization resistance to opposite across	Ortumstic
pathogens	
4.7 Summary of results	69
5. DISCUSSION	71
5.1.1 Conclusions on prevention of coprophagy in mice during homeostasis and infection.	
5.1.2 Limitations and Outlook.	
5.2.1 Conclusions on ampicillin-resistant bacterial consortia	
5.2.2 Limitations and Outlook	/ /
6 DECEDENCES	70

LIST OF FIGURES

Figure 3.1 Construction and use of functional tail cup devices to prevent coprophagia in mice
Figure 3.2 Prevention of coprophagia leads to a loss of anaerobic bacteria in the upper GI tract
Figure 3.3 Coprophagia increases the concentrations of free amino acids in the small intestine
Figure 3.4 Coprophagia increases the abundance of both host and microbially-modified metabolites in the SI
Figure 3.5 Preventing coprophagia in mice leads to a reduction in the stimulation of the intestinal immune system
Figure 3.6 Coprophagia prolongs infection with VRE, but is not required to colonize the antibiotic-treated SI
Figure 3.7 Recovery of Reg3g expression after ampicillin-treatment in non-coprophagic mice is sufficient to clear VRE from the small intestine and reduce VRE in the colon39
Figure 3.8 Enterococcus faecium forms small clusters along the SI epithelium41
Figure 3.9 Non-coprophagic mice have increased Ef-GFP+ clusters in their ileum43
Figure 4.1 One out of the seven different microbiota tested were resistant to ampicillin-induced dysbiosis
Figure 4.2 Ampicillin-resistant microbiota retain production of most bile acid and short chain fatty acid metabolite compounds after perturbation with ampicillin
Figure 4.3 The ampicillin-resistant phenotype is found in only a few bacteria from the ampicillin-resistant microbiota of mouse group H47
Figure 4.4 Ampicillin-resistant bacteria isolated from the fecal microbiota of mouse group H47
Figure 4.5 Ampicillin-resistant bacteria isolated from the fecal microbiota of the ampicillin-resistant microbiota (ARM) described in Caballero et al
Figure 4.6 Structure of the putative <i>bla</i> CLO1 gene operon from <i>Enterocloster bolteae</i> _{H47} 61
Figure 4.7 Beta-lactamase genes from ampicillin-resistant bacteria isolated from the fecal microbiota of mouse group H47

Figure 4.8 Resistance to ampicillin-mediated dysbiosis enables resistance to infection	65
Figure 4.9 Suppression of VRE growth <i>in vitro</i> by bacterial isolates from the fecal microwse group's H47 and ARM	
Figure 4.10 Bacterial isolates from the fecal microbiota of group H47 protect against a induced dysbiosis and subsequent VRE infection	1

LIST OF TABLES

<u>ACKNOWLEDGEMENTS</u>

I would first like to thank my mentor, Eric Pamer. Thank you for always challenging me to think deeply, and for always supporting me in my quest for independence. It's been really inspiring watching you build the DFI from the ground up, and your vision for science and health has greatly impacted how I approach research. And thank you for reminding me to slow down sometimes.

Thank you to my thesis committee Sam Light, Tanya Golovkina, and Alexander Chervonksy. My time in grad school had a lot of ups and downs, and your consistent guidance through it all was incredibly helpful. Thank you to all of you for being so kind whilst still pushing me to work my hardest, I wouldn't have managed to get all of this done without your unwavering support.

Thank you to everyone in my lab, especially my fellow grad students Cody and Sophie. It's been so fun having people in the exact same phase of grad school as you to go through it all together. And a special thank you to Sophie for helping me do so many of the experiments, as well as for being one of the best friends that I made in grad school. I also want to thank everyone in the DFI, from grad students in the other labs to all of the team members of the cores, you all have made working in the lab such a joy. Whether we were troubleshooting an experiment or just gossiping, I really cherish all of the chats we've had over the years while you grabbed coffee or water.

And thank you to everyone in the immunology and microbiology communities here at UChicago. I'm so lucky to have gotten to know the kindest and most brilliant scientists during my time here. I'm a much better scientist today than I was 6 years ago, and it is thanks to the outstanding training I've received from the Committee on Immunology. I also want to thank the

friends I've made in grad school beyond just my program, thanks to Sandra's Survivor nights and my time as a union organizer. You all brought so much joy to this period of my life, and I can't thank you enough. And thank you to my comrade Thea, who managed to make microscopy fun.

None of this would have been possible without the support of my family. Without the help and encouragement of you all, I would have never left Oklahoma and truly challenged myself to accomplish what I wanted. I especially want to thank my husband, Mark. Without you holding me together, I would have fallen apart before making it this far. Thank you for always taking care of me, as well as our cats Kwacha and Lulu. You'll never know how much your love and support truly means to me, but I'll spend forever doing my best to show you.

ABSTRACT

A common side effect of antibiotic treatment is the depletion of the patient's endogenous gut microbiota, which provides critical protection from antibiotic-resistant pathogens that commonly contaminate hospitals, such as vancomycin-resistant *Enterococcus* (VRE).

Understanding mechanisms of colonization resistance to VRE are therefore critical for the development of therapeutic interventions for patients undergoing antibiotic therapy. In this work, we took 2 different approaches to investigate how colonization resistance is formed by the commensal microbiota to protect the host.

In the first approach, we utilized a recently designed tail cup device that functioned to prevent coprophagia during mouse experiments, enabling us to study the dynamics of VRE colonization without the influence of pathogen recycling. We found that VRE was capable of engrafting into the small intestine (SI) of antibiotic-treated mice even when coprophagia was prevented. Using a green-fluorescent protein expressing strain of *Enterococcus faecium*, we visualized the association of E. faecium in the SI of non-coprophagic mice and found small clusters of bacteria colonizing the epithelium directly. Application of these tail cups also allowed us to characterize how the large intestinal microbiota influences the immune system in the SI, increasing the stimulation of Reg3g production in the ileum and skewing the helper T cell populations of the mesenteric lymph nodes towards increased Th17 cells. Despite this, mice in tail cups were able to resolve VRE infection earlier than mice in mock cups, suggesting that the less diverse microbiota of their SI and subsequent decreased immune stimulation was still sufficient to confer protection from VRE when pathogen recycling is inhibited. Conversely, the increased stimulation and bacteria present in the coprophagic mice was less efficient at clearing VRE from the GI tract, likely due to the extremely high loads of VRE consumed during the

course of infection. These studies indicate that VRE is quite sensitive to the resistance conferred by the SI immune system and microbiota, and that de-colonization of this area precedes clearance of the large intestine.

In our second approach, we investigated ampicillin-resistance in antibiotic-naïve gut microbiota. By using commercially available mouse colonies, we were able to assess the presence of resistance to antibiotic treatment in healthy microbiota with no history of infection or antibiotic usage. Of the 7 different colonies we tested, we found that 1 was resistant to ampicillin-induced dysbiosis, enabling resistance to subsequent infection with VRE. We isolated 3 bacteria from the resistant microbiota, and demonstrated that they are sufficient to confer protection to an antibiotic-sensitive microbiota. These findings demonstrate that ampicillin-resistance can be found in diverse, complex microbiota derived from healthy populations unexposed to antibiotics. Altogether, this project brings insights into mechanisms of indirect resistance to colonization by VRE, showing that the SI is a distinct niche for colonization, and demonstrating the potential therapeutic role for antibiotic-resistant commensals.

CHAPTER 1: Introduction

1.1 Vancomycin-resistant Enterococcus faecium (VRE)

The hospital environment creates a uniquely hazardous breeding ground for multidrug resistant bacterial pathogens. Many infections with multidrug resistant pathogens originate in the gastrointestinal (GI) tract, including vancomycin-resistant *Enterococcus* (VRE) infection, a Gram-positive facultative anaerobic bacterium highly associated with hospital-acquired infections¹. The healthy intestine is not typically susceptible to infection with VRE due to colonization resistance, the process by which the microbiota provides protection from pathogens². However, during circumstances that perturb the microbiome, such as treatment with antibiotics, colonization resistance is lost, and patients become highly vulnerable to intestinal domination with VRE³. Intestinal domination has been shown to precede bloodstream infection⁴, and is associated with worse outcomes in stem cell transplant patients⁵. Understanding mechanisms of colonization resistance to VRE are therefore critical for the development of therapeutic interventions for vulnerable patients.

Antibiotic-resistant *Enterococcus faecalis* (*E. faecalis*) was first identified as a causative factor of endocarditis in the 1970s, with the intrinsic resistance of the bacteria leading to issues even early on with finding effective treatments¹. A few decades later, multi-drug resistant *E. faecium* began to be isolated from patient infections⁶. Despite being etiological agents of the same types of infections, these 2 species of enterococci are quite genetically distinct; they are more closely related to other harmless enterococcal species than they are to each other⁷. Other

species of *E. faeciu*m and *E. faecalis* outside of the pathogenic clades are normal commensals gut microbes that do not dominate the intestine⁸.

Unlike some pathogenic bacteria in the intestine, such as *E. coli* and *C. difficile*,

Enterococcus does not produce any toxins that directly target the gut epithelium and lead to host damage and ensuing inflammation in the gut⁹. Instead, the pathogenic qualities of the

Enterococcus isolates have typically been associated with their ability to efficiently colonize and achieve high density in the intestine of vulnerable patients ^{10,11}. Other factors associated with virulence that have been identified include secreted factors that help with biofilm formation, and cell surface components that likely interact with the host cells⁶. However, these factors are not specific to species isolated in infections, and instead are common amongst gut-residing enterococcal species.

The success of *Enterococcus faecium* as an opportunistic pathogen lies more in its ability to quickly dominate the gut of patients undergoing dysbiosis. Inoculation of a single CFU of VRE into antibiotic-treated mice showed rapid domination of their fecal microbiota.

Furthermore, the VRE isolate evolved continuously in the intestinal niche, showing expansion and extinction of multiple SNVs throughout the course of the experiment, including a SNV that increased resistance to the ampicillin treatment¹². These findings demonstrate how quickly VRE can adapt to the intestinal niche. The diversification of VRE isolates also suggests that there are potentially multiple niches throughout the gut that VRE is adapting to.

1.2 Colonization resistance to VRE

Colonization resistance mechanisms can be broadly divided into two categories: direct and indirect², ¹³. Direct colonization resistance refers to mechanisms that involve direct interactions between the commensal microbiota and the pathogen, such as modification of secondary bile acids that inhibit *C. difficile*¹⁴. In contrast, indirect colonization resistance mechanisms are immune-mediated mechanisms of pathogen inhibition that are induced by the commensal microbiome, such as the stimulation of the antimicrobial C-type lectin RegIIIgamma (Reg3g) to protect against *Listeria monocytogenes* infection¹⁵.

There are many different mechanisms through which the commensal microbiome forms colonization resistance to VRE specifically. Our lab previously identified a consortium of bacteria that provides direct resistance to VRE through production of a lantibiotic peptide that can directly kill VRE¹⁶. This consortium was isolated from a mouse colony that had developed an ampicillin-resistant microbiota (ARM) after 2 decades of treatment with a beta-lactam antibiotic in their drinking water¹⁷.

1.3 Influence of the gut microbiota and metabolites on the intestinal immune system

To coordinate the response of the immune system to the commensal microbiota, it is critical for the epithelium to recognize and respond to the presence of the microbiota. The innate immune system detects the microbiota through stimulation of pattern recognition receptors (PRRs), such as Toll-like receptors (TLRs) which are transmembrane receptors that recognize

conserved microbial components present on both commensal microbes and pathogens¹⁸.

Previous studies from the Pamer lab have identified TLR stimulation by the microbiota to be a critical inducer of Reg3g in the small intestine (SI). Reg3g can be stimulated by LPS stimulation of TLR4¹⁵, flagellin stimulation of TLR5¹⁹, and double-stranded RNA stimulation of TLR7²⁰. The lectin Reg3g is secreted directly by the small intestinal epithelium, and it can directly kill VRE in the ileum²¹. Production of Reg3g can also be induced by host cytokine production of interleukin-22, which is mainly produced by ILC3s²².

Increasing attention has been given to the role that microbially conjugated bile acids play in host physiology. Primary bile acids (PBAs) are molecules derived from cholesterol by the host that are essential for the digestion of dietary fats²³. After synthesis in the liver and subsequent release into the duodenum via the gallbladder, the vast majority of bile acids are re-absorbed into the SI. However, a small proportion continue on to the colon, where they are further modified by commensal bacteria²⁴. This conversion of primary bile acids into secondary bile acids (SBAs) has been shown to have dramatic consequences on the health of the host²⁵. For example, germination of *Clostridoides difficile* spores is inhibited by the presence of secondary bile acids, protecting the host from infection¹⁴.

Some bile acids have also been implicated in the differentiation of naïve conventional CD4+ T (Tconv) cells into regulatory T cells (Tregs) of the gut. Researchers have shown that derivatives of lithocholic acid (LCA) can directly influence the identity of Tconv cells. One derivative, 3-oxoLCA, inhibits the T helper 17 (Th17) transcriptional program through direct binding of the key transcription factor RORgt²⁶. Another derivative of LCA, isoalloLCA, directly enhances the differentiation of Tconv cells into to Treg cells through its actions on the nuclear hormone receptor NR4A1²⁷. Removal of secondary bile acids from the host reduces the

pool of colonic RORgt+ Tregs, which can exacerbate inflammation in the intestine²⁸. Aside from the ability of bile acids to directly influence Tconv cell differentiation, research has also found that they can also influence other immune cells that promote T cell activation. The secondary bile acid 3β-hydroxydeoxycholic acid (isoDCA) promotes Treg development via inhibitory effects on dendritic cells (DCs), thus preventing them from promoting inflammatory T cell phenotypes²⁷. The ability for the microbiota to induce Tregs is critical for maintaining tolerance to the microbiome and preventing excessive inflammation in response to commensals²⁹. These findings illustrate how metabolites from the microbiota can directly influence intestinal homeostasis for the benefit of both the host and the microbes.

Certain gut microbes are critical for the induction of pTregs in the gut, and without their generation, naïve CD4+ T cells instead differentiate into more inflammatory T helper 17 (Th17) and Th1 cells³⁰. Further investigations have demonstrated that microbiota-induced Tregs often co-express RORgt, a transcription factor characteristic of Th17 cells, in a manner that is dependent on microbial activation of intestinal dendritic cells (DCs)^{31,32}. These microbiota-induced Rorgt+Foxp3+ Tregs are essential for suppression of Rorgt+ Th17 cells, and occur at much lower frequencies in the absence of the microbiome³³. Analysis of the specificity of intestinal Tregs has shown that they are largely specific for microbiota-derived antigens, and do not overlap much in specificity with other effector T cells in the colon nor Tregs sampled from other organ sites³⁴. Altogether, these studies demonstrate how the intestinal immune system is in constant dialogue with the gut microbiota to coordinate protective responses against invading pathobionts.

Considerable efforts have been made to develop therapeutic treatments that neutralize the harmful side effects of antibiotics on the commensal bacteria in the intestine. For example, researchers have developed a purified beta-lactamase to give to patients to help remove the antibiotics from their intestinal lumen³⁵. Mechanisms of resistance to beta-lactams in anaerobic bacteria include production of inactivating enzymes (beta-lactamases), alteration of penicillin-binding proteins, and blocking penetration of the antibiotic. However, the most common mechanisms is beta-lactamase production³⁶.

Another group has demonstrated that a commensal species engineered to express a betalactamase was able to breakdown ampicillin in the gut of mice and shield the commensal gut microbiota from infection³⁷, illustrating the potential for probiotics to be utilized as a tool to protect the healthy bacteria that were in the gut before it becomes irreparably damaged by their antibiotic treatment regimen.

Rather than engineering new functional properties into bacteria, we can take advantage of the diversity of functions that already exist in bacteria that are apart of native gut ecosystems³⁸. A major advantage of this approach is that these bacteria evolved to perform these functions already in the context of the complex gut microbial niche³⁹, making it easier to predict how these bacteria will function when given to patients. Our lab has previously isolated a 4-member consortium of bacteria from an in-house mouse colony with an ampicillin-resistant microbiota (ARM) that rendered ampicillin-treated mice resistant to colonization with VRE¹⁷. Bacterial members of this consortium degraded ampicillin, allowing the consortium to survive during antibiotic treatment¹⁷, and secreted a lantibiotic potently active against VRE¹⁶.

1.5 Summary of project rationale

The objectives of this thesis are to 1) characterize the dynamics of VRE infection in the SI of non-coprophagic mice and 2) identify ampicillin-resistant commensal bacteria that can protect from VRE infection. The overall goal of this work is to understand how the gut microbiota provides colonization resistance to VRE, providing new avenues for the development of future probiotic therapies. Disentangling the colonization dynamics of the small intestine (SI) vs. the large intestine will provide valuable insights for designing consortia that can uniquely target these areas. This will enable the eradication of VRE from the entire GI tract, thus preventing recurrent infection or further organ dissemination in patients. This work also provides a framework for the investigation into ampicillin-resistant microbiota in healthy, antibiotic-naïve samples, through demonstration that only a few bacteria are required to recreate resistance phenotypes and protect from VRE challenge. Altogether, these experiments define different mechanisms through which the gut microbiota provide colonization resistance to VRE infection, bringing insights into indirect resistance mechanisms including resilience against ampicillin and induction of antimicrobial peptides in the SI.

CHAPTER 2: Materials and Methods

2.1 Experimental model and subject details

2.1.1 Mouse subjects

All mouse studies were approved by The University of Chicago Institutional Animal Care and Use Committee (protocol 72599). 6–8-week-old female C57BL/6 (B6) mice were ordered from the AX8, AX4, EM05, and RB15 mouse colony breeding rooms from Jackson Laboratories, and the H47, K92, and R07 mouse colony breeding rooms from Charles River Laboratory, and were fed a standard chow diet and given autoclaved acidified drinking water. Germ-free (GF) B6 mice were bred in house in plastic isolators at the University of Chicago's Gnotobiotic Research Animal Facility, and were fed autoclaved food and sterile water. GF mice were transferred into sterile, individually ventilated cages after association with bacteria, where they remained housed for the duration of the experiment. During experiments, all mice were housed in BSL2 facilities under specific-pathogen-free conditions at the University of Chicago. All mice were randomized and single housed in cages containing corncob bedding.

2.1.2 Tail cups and mock cups

Tail cups were designed according to published protocol⁴⁰. Briefly, a rotary tool was used to cut a 20 mL syringe and drill a hole into the end, as well as small holes on the side to encourage desiccation of the fecal pellet. Tail sheaths were fashioned from silicone hose, and a metal washer was glued to the end of the syringe to build the "cup". For mock cups, the sides of the syringe were cut off, allowing fecal pellets to fall back into the cage. Upon initial application, a small amount of tissue adhesive is applied to the base of the tail, then the silicone sheath is

glued on. Mice are left alone in their cage for 1-2 minutes while adhesive dries, and then functional or non-functional mock cups are slipped over the silicone sheath, where they rest on an indention carved into the sheath. Tail cups are emptied once daily, mock cups have their cups briefly removed daily as well. For weight collection, after removal of cups mice are placed into sterile cups, then weighed.

2.1.3 Ampicillin Treatment

Mice were treated with 0.5 g/L ampicillin (Athenex NDC: 70860-118-99) mixed with their autoclaved acidified drinking water. Ampicillin was refreshed every 3-4 days due to degradation.

2.1.4 Bacterial isolates from human donors

Human bacterial isolates containing similar beta-lactamase genes were identified using the DFI Symbiotic Biobank website, and genomes are also available in the NCBI RefSeq database. The DFI Symbiotic Biobank is commensal bacterial strain bank of gut bacteria isolated from 21 healthy human fecal donors. Collection of these samples, isolation of bacteria, and genetic analyses performed described previously.

2.1.5 Infection Models

Mice were challenged via oral gavage with approximately 10⁵ CFUs of VRE (*E. faecium*, ATCC 700221), CRKp (K. pneumoniae MH258), or Ef-GFP+ (*E. faecium*_{com15}-GFP+, gift from Howard Hang @ Scripps) suspended in 200 μL of phosphate buffered saline. Fecal samples were collected from mice prior to infection and on the indicated days post-infection.

2.1.6 Fecal microbiota transplant (FMT) into germ-free (GF) mice

Fecal pellets were collected from antibiotic-naïve AX8 mice and resuspended in 1mL of 20% glycerol mixed with DPBS per 25mg of feces. Fecal suspensions were then split, with half of the samples getting mixed with the 3 extra bacteria isolated from the H47 fecal microbiota. Aliquots of both inocula mixtures were then stored at -80C until ready for use. Samples were thawed on ice immediately before inoculation into mice by oral gavage. Mice were given 200 µL of either inoculum 1x/day for 3 consecutive days.

2.2 Experimental method details

2.2.1 16S rRNA gene sequencing and analysis

performed using Qubit and Tapestation and sequenced on Illumina MiSeq platform to generate 2x250bp paired-end reads. For 16S rRNA gene amplicon sequence analysis, we used DADA2 (v1.18.0)84 as our default pipeline for processing MiSeq 16S rRNA gene reads with minor modifications in R (v4.0.3). Specifically, reads were first trimmed at 210 bp for forward reads and 150 for reverse reads to remove low quality nucleotides. Chimeras were detected and removed using the default consensus method in the DADA2 pipeline. Then, ASVs with length between 300 bp and 360 bp were kept and deemed as high quality ASVs. Taxonomy of the resultant ASVs were assigned to the genus level using the RDP classifier (v2.13)86 with a minimum bootstrap confidence score of 80. Results were analyzed as using the Phyloseq(v.1.46.0) R package, Shannon index scores were calculated using the estimate richness() function, Bray-Curtis dissimilarity was calculated and plotted in R using the ordinate() and plot ordination() functions, bar plots made using ggplot2 package.

2.2.2 16S rRNA gene qPCR

An aliquot of the samples prepared for 16S rRNA gene sequencing were diluted to 20 ng/μL. The primers 563F (5'-AYTGGGYDTAAAGNG-3') and 926R (5'-CCGTCAATTYHTTTRAGT-3') for the V4-V5 region of the 16S rRNA gene were used for amplification. A standard curve was created with a V4-V5 region on a linearized TOPO pcr2.1TA vector isolated from Eschericha coli DH5α cells. The vector was serially diluted 5-fold ranging from 108 to 103 copies/μL. qPCR was performed on a QuantStudio 6 Pro (Applied Biosystems) using PowerTrack SYBR Green Master Mix (A46109) with the following cycling conditions: 95°C for 10 min, followed by 40 cycles of 95°C for 30 s, 52°C for 30 s,and 72°C for 1 min. Design and Analysis v2 software was used to calculate the copy numbers for each sample.

Copy numbers were normalized based on the weight of fecal pellets the DNA was extracted from.

2.2.3 Quantitative and qualitative metabolomics

Mouse fecal pellets were collected in 2 mL cryo-microcentrifuge tubes (Sarstedt 72.694.006) on collection days and placed on dry ice until transferred to a -80°C freezer until sequenced. Fecal samples were weighed and extraction solvent, 80% methanol spiked with internal standards, was added to make a ratio of 100 mg of material/mL of extraction solvent. Samples were then homogenized at 4°C using a Bead Mill 24 Homogenizer (Fisher; 15-340-163) set at 1.6 m/s with 6 thirty-second cycles, 5 seconds off per cycle. Next, samples were centrifuged at -10°C, 20,000 x g for 15 minutes. The supernatant was used for subsequent metabolomic analysis. Short-chain fatty acids (SCFAs) and 5-aminovalerate were quantified via derivatization with pentafluorobenzl-bromide (PFBBr). Methanol containing internal standards was added to fecal samples at 4 volumes per a milligram of feces. Samples were centrifuged followed by the addition of x µL borate buffer at a pH of 10. Next, 150 mM PFBBr suspended in methanol cyanide (acetonitrile) was added to the samples and incubated at 65°C for 1 hour. Lastly, hexanes were extracted and subjected to gas chromatography-mass spectrometry (GC-MS) (Agilent 8890/5977B and 7890B/5977B) with chemical ionization and negative mode detection. Bile acids and ampicillin were quantified via liquid chromatography-mass spectrometry (LC-MS). 75 µL was added to mass spectrometry autosampler vials (Microliter; 09-1200) and subsequently dried using a nitrogen stream of 30 L/min (top) and 1 L/min (bottom) at 30°C (Biotage SPE Dry 96 Dual; 3579M). Dried samples were then re-suspended in 750 µL of a 50:50 water:methanol mixture. The vials were added to a thermomixer (Eppendorf) to resuspend analytes under the following conditions: 4°C, 1000 rpm for 15 min with infinite hold at 4°C. To remove insoluble debris, samples were centrifuged in microcentrifuge tubes at 20,000 x g for 15 mins at 4°C. 700 µL was transferred to a new mass spectrometry autosampler vial and analyzed in negative mode on a liquid chromatography system (Agilent 1290 infinity II) coupled to a quadrupole time-of-flight (QTOF) mass spectrometer (Agilent 6546) equipped with an Agilent Jet Stream Electrospray Ionization source. 5 µL of sample was then injected onto an XBridge BEH C18 column (3.5 μm, 2.1 x 100 mm; Waters Corporation, PN) fitted with an XBridge BEH C18 guard (Waters Corportation, PN) at 45°C. Elution started with 72% A (Water, 0.1% formic acid) and 28% B (Acetone, 0.1% formic acid) with a flow rate of 0.4 mL/min for 1 min and linearly increased to 33% B over 5 min, then linearly increased to 65% B over 14 min. Then the flow rate was increased to 0.6 mL/min and B was increased to 98% over 0.5 min and these conditions were held constant for 3.5 min. Finally, re-equilibration at a flow rate of 0.4 mL/min of 28% B was performed for 3 min. The electrospray ionization conditions were set with the capillary voltage at 3.5 kV, nozzle voltage at 2 kV, and detection window set to 100-1700 m/z with continuous infusion of a reference mass (Agilent ESI TOF Biopolymer Analysis Reference Mix) for mass calibration. A 10-point calibration curve was used for quantification. Data analysis was performed using MassHunter Profinder Analysis software (version B.10, Agilent Technologies) and confirmed by comparison with authentic standards. Normalized peak areas were calculated by dividing raw peak areas of targeted analytes by averaged raw peak areas of internal standards.

2.2.4 Reg3g quantification from the ileum

1 cm of distal ileum per mouse was harvested in Trizol (Roche) and RNA was prepared according to the manufacturers' protocols. RNA was DNase treated (Roche) and cDNA was reverse transcribed using High-Capacity cDNA Reverse Transcription Kit (Applied Biosystems). cDNA was used as template in a real time PCR reaction using Taqman primer-probes sets on a QuantStudio6. cDNA was semi-quantitated using the $\Delta\Delta$ CT method with Hprt (mouse) as an internal control for all samples.

2.2.5 Quantification of pathogen burden

Samples collected from VRE infected mice were diluted 10-fold in PBS and plated onto Difco Enterococcosel agar (supplemented with 8 mg/ml vancomycin; Novaplus and 100 mg/ml streptomycin; Fisher) and incubated at 37°C for 24 hrs. Efcom15-GFP+ samples were quantified the same way, but with no antibiotic supplement. Fecal samples collected from CRKp infected mice were diluted 10-fold in PBS and plated onto LB agar supplemented with 100 μg/mL carbenicillin (Fisher BioReagents BP2648) and 50 μg/mL neomycin, and incubated at 37°C for 24 hrs. CFUs were then counted and normalized to fecal mass.

2.2.6 Microscopy imaging and analysis

Samples were collected from Ef-GFP+ monocolonized mice 2 weeks post-infection.

Distal ileum and colon samples were flushed of luminal contents with sterile PBS, then fixed in 2% paraformaldehyde for 20 minutes at room temperature. Samples were then stained with Hoescht and anti-mouse CD326-AlexaFluor594 (Biolegend) for 20 minutes, then sliced into 2mm thick sections, then mounted onto slides (18-well glass bottom, Ibidi) with mounting

medium (Ibidi). 300um z-stacks were imaged from each section at 20x on a SoRa Marianas Spinning Disk Confocal. 7 slices were taken from every sample, each at 50um apart. Tiles stitched using Slidebook 2025, max Z projections made using ImageJ. 3 regions of interest (100x100um) were drawn onto Ef-GFP+ clusters, then quantification was done using ImageJ macros.

2.2.7 Shallow shotgun sequencing and analysis

Bacterial DNA was extracted using the QIAamp PowerFecal Pro DNA kit (Qiagen). Prior to extraction, samples were subjected to mechanical disruption using a bead beating method. Briefly, samples were suspended in a bead tube (Qiagen) along with lysis buffer CD1 and loaded on a bead mill homogenizer (Fisherbrand). Samples were then centrifuged, and supernatant was resuspended in CD2, a reagent that effectively removes inhibitors by precipitating non-DNA organic and inorganic materials including polysaccharides, cell debris and proteins. DNA was then purified routinely using a spin column filter membrane and quantified using Qubit (Life Technologies). Libraries were prepared using 200 ng of genomic DNA using the QIAseq FX DNA library kit (Qiagen). Briefly, DNA was fragmented enzymatically using a nuclease into shorter fragments and desired insert size was achieved by adjusting fragmentation conditions. Fragmented DNA was end repaired to generate blunt end fragments using a T4 DNA polymerase, and 'A's' were added to the 3'ends to stage inserts for ligation. During ligation step (blunt end AT ligation), Illumina compatible Unique Dual Index (UDI) adapters were added to the inserts and prepared library was PCR amplified. Amplified libraries were recovered using magnetic beads, and QC was performed using Tapestation 4200 (Agilent Technologies). Libraries were sequenced on the Illumina HiSEq platform. This

produced approximately 7-8 million paired-end reads for each sample with a read length of 150 bp. After trimming adapters from raw reads, the quality of reads was assessed and controlled with Trimmomatic38 (version 0.39). Reads that map to the mouse genome were removed with kneaddata (version 0.7.10). All reads were then assembled into contigs using MEGAHIT39 (version 1.2.9). In order to assign taxonomy, the filtered reads were run through MetaPhlAn4.30. Multivariable linear models were fit using MaAsLin2 (version 1.14.1) to identify associations between bacterial taxonomy and mouse group origin. Features were log-transformed and normalized; FDR < 0.05 was used to identify significant associations which were plotted using ggplot2 R package.

2.2.8 Ampicillin-resistance testing of the fecal microbiota

A fecal pellet was collected from an ampicillin-treated H47 mice, and dissociated anaerobically in DPBS. The H47 fecal suspension was diluted 10⁻⁵-fold, then 100 uL were plated onto BHI agar supplemented with L-cysteine (1.0 g/L) and yeast-extract (5.0 g/L) containing various concentrations of ampicillin. Plates were incubated anaerobically at 37°C for 2 days, after which plates were scraped. Scrapings from plates of the same ampicillin concentration were pooled together, then submitted for 16s-sequencing.

2.2.9 Isolation of bacteria from H47 fecal microbiota

To isolate bacteria from H47 fecal pellets, feces were diluted to 10-5 and then plated onto supplemented BHI containing ampicillin or LKV plates. Colonies were picked and streaked onto fresh agar to ensure purity. Isolated clones were resuspended in PBS plus glycerol (20%) and stored at -80°C. Full-length 16S rRNA genes were amplified by colony PCR using primers 8F

(50-AGAGTTTGATCCTGGCTCAG-30) and 1492R (50-GGTTACCTTGTTACGACTT-30). The resulting PCR product was Sanger sequenced with primers spanning the full 16S gene (8F and 1492R) as well as primers specific to the V4-V5 region (517F, 50-GCCAGCAGCCGCGGTAA-30) and classified using BLAST (98%–100% sequence identity). For augmentation of FMT, bacteria were individually cultured on Columbia plus 5% sheep blood agar (BD Biosciences) for 2 days at 37°C under anaerobic conditions, plate cultures were scraped and resuspended in PBS, mixed in a 1:1 ratio (10⁵-10⁶ CFU per isolate), then added to the AX8 fecal suspension.

2.2.10 Isolate susceptibility to ampicillin and beta-lactamase detection assay

To determine MIC of ampicillin for bacterial isolates, bacteria was cultured anaerobically at 37°C in BHIS containing ampicillin. Optical density was then measured at 600nm after 24 hours. For detection of beta-lactamases, bacterial isolates were cultured under the same conditions but for 3 days, then 100 μL of each culture were added to a 96-well plate, followed by the addition with 3 μL of nitrocefin (0.2 mg/ml, Fisher). After 20 mins of incubation at room temperature while protected from light, supernatants were taken from plates and then optical density at 490 nm was read. To compare bacterial isolates from previously studied consortia, frozen stocks for *Enterocloster bolteae*_{ARM}, *Bacteroides sartorii*_{ARM}, and *Parabacteroides distasonis*_{ARM}, were cultured and tested in the same manner.

2.2.11 Whole-genome shotgun sequencing and assembly

Bacterial DNA was extracted using the QIAamp PowerFecal Pro DNA kit (Qiagen).

Libraries were sequenced on an Illumina MiSeq to generate 2x250bp, targeted for 1 to 3 million

pair-end reads per sample. Adapters were trimmed with Trimmomatic82 using following parameters: the leading and trailing 3 bp of the sequences were trimmed off, quality was controlled by a sliding window of 4, with an average quality of 15. Moreover, any read that was less than 50 bp long after trimming and quality control were discarded. The remaining high-quality reads were assembled into contigs using SPAdes (v.3.14.0).83

2.2.12 Identification of beta-lactamase genes in bacterial isolate genomes

Putative beta-lactamase gene sequences in H47 isolate genomes were detected using the tBLASTn program from the BLAST (v 2.13.0+ suite90) with settings against all beta-lactamase gene sequences found in CARD and the NCBI Pathogen Detection Reference Gene Catalog. The BLASTn output was further parsed to filter low confidence hits The gene segments identified by BLASTn were retrieved using BEDtools, then translated using the EMBOSS -getorf function. HMMER was used to validate the presence of conserved beta-lactamase Pfam domains in these segments. Annotation of nearby gene domains in the *E. bolteae*H47 genome was also done using HMMER search for Pfam domains. Gene operon diagram constructed using Geneius.

2.2.13 Analysis of beta-lactamase genes in metagenomic reads

Beta-lactamase gene sequences from the H47 bacterial isolates were built into a bowtie2 index, then bowtie2 was used to recruit trimmed and host-filtered short reads from fecal metagenomic samples. Samtools was used to convert resulting SAM files to BAM files, then sort and index them. The idxstats function was then used to determine the total reads mapped to each gene per sample, which was then used to calculate the mapped reads per kilobase per million (RPKM).

2.2.14 Assessment of genes in other bacterial genomes

Beta-lactamase gene sequences from the H47 bacterial isolates were queried against the bacterial genomes of all human isolates in the the DFI Symbiotic Biobank using the BLASTx function on the website. The genomes of isolates with matches were downloaded, then BEDtools was used to retrieve the matching sequences. Sequences were aligned using the MAFFT program, using the parameters -max_iterations 1000. The resulting alignment output was then input into IQ-TREE to build a maximum likelihood tree with settings -m TEST, -bb 1000, -nt AUTO. The output treefile was then visualized using ggplot2 in R.

2.2.15 In vitro VRE Competition/Suppression Assay with isolates

BHI. For co-culture tests, stationary phase cultures of bacterial isolates were normalized to the same OD, and then ~100 CFUs of VRE was added to 1 mL of each culture. For supernatant test, 1 mL of supernatant from stationary phase cultures of bacterial isolates was inoculated with ~100 CFUs of VRE. After being incubated anaerobically overnight at 37°C, cultures were diluted 10-fold, plated onto Difco Enterococcosel agar, and then incubated overnight at 37°C for enumeration of VRE CFUs.

2.3 Quantification and statistical analysis

Statistical analyses were performed using Graph-Pad Prism (version 6.0), and R (v4.3.3). Data are expressed as mean \pm SEM. The statistical parameters for each experiment are detailed in the Figure legends. For the Student's t test, Mann-Whitney test and Spearman's correlation

test, P values < 0.05 were considered significant. The Benjamini-Hochberg method was applied to control for false discovery rate. No assumption on the distribution of the data were made, and only nonparametric statistical tests were used.

CHAPTER 3: Prevention of coprophagia in mice enables full resolution of the biogeographic distribution of the intestinal microbiota at homeostasis and during infection with VRE

3.1 Introduction

The commensal gut microbiota can provide colonization resistance to pathogens in an indirect form via activation of the host's protective immune responses². The majority of the immune cells of the intestine are localized in the small intestine, as well as many specialized epithelial cells that also actively participate in host defense³⁰. For example, former research from the Pamer lab has demonstrated that the commensal microbiota is critical for stimulation of the host C-type lectin RegIIIgamma (Reg3g) from the ileal epithelium ^{19,20}. Using an ligated ileal loop model, it was demonstrated that the induction of Reg3g by bacterial LPS was sufficient to reduce the amount of VRE in the ileum²¹. These findings suggest that the small intestine (SI) is a discrete niche where the microbiota forms colonization resistance to VRE. However, whether VRE is a pathogen that truly colonizes and dominates the SI during its pathogenesis in the intestine remains unclear. An obstacle to studying the dynamics of intestinal VRE colonization in the SI using experimental models has been coprophagia by colonized mice, which results in reinoculation with fecally-shed bacteria (Figure 3.1A). Coprophagia refers to the ingestion by an animal of excrement, and mice engage in both autocoprophagia (ingestion of their own feces) as well as allocoprophagia (ingestion of feces from other mice)⁴¹. In rodents, coprophagy enables the acquisition and absorption of nutrients in the SI that are synthesized in the large intestine (LI) by anaerobic bacteria⁴¹. Thus, it remains to be determined whether the SI represents a niche for

VRE colonization, and how colonization resistance is formed there in comparison to the LI. To remove this variable from our infection models and properly characterize the niche-specific

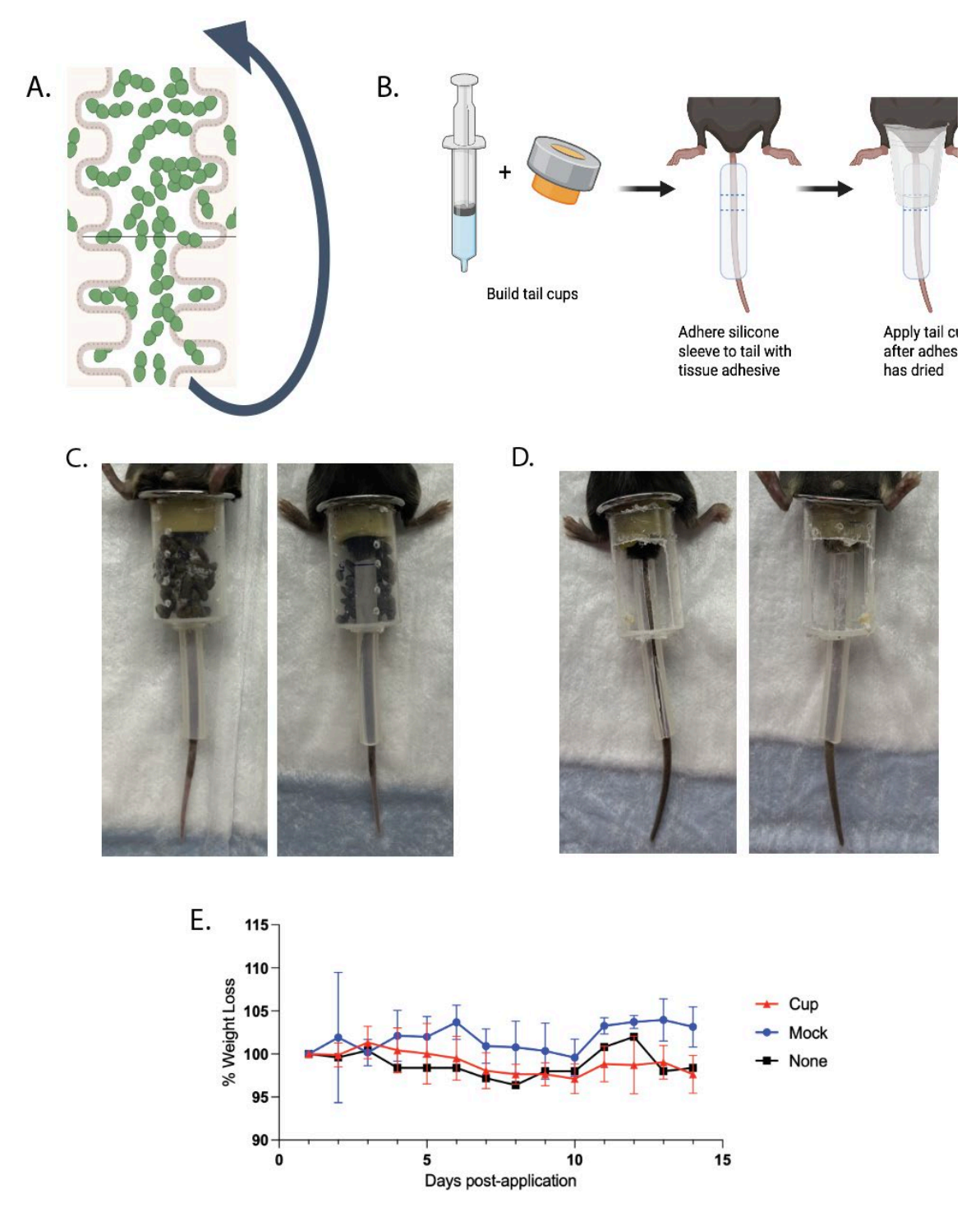


Figure 3.1 Construction and use of functional tail cup devices to prevent coprophagia in mice A. Model of pathogen recycling in standard mouse experimental mouse models. B. Schematic of build and application of functional tail cups that prevent coprophagia.

Figure 3.1 (continued) C. Functional tail cup and **D.** non-functional mock cups in use. **E.** Percentage of weight lost by each mouse throughout the experiment. Mice were weighed once a day, without the tail cup devices on. Mice outfitted with functional tail cup devices (Cup) are represented by red triangles, and mice outfitted with non-functional mock cup devices (Mock) are represented by blue circles. A control mouse with no cup on was included, shown as a black square. Each line represents 3 mice.

colonization dynamics of VRE, we made use of a previously designed functional tail cup device to prevent coprophagia⁴⁰. By outfitting mice with these tail cup devices prior to infection with VRE (**Figure 3.1**), we were able to study the dynamics of VRE in the SI in a setting much closer to human physiology.

3.2 Construction and use of functional tail cup devices to prevent coprophagia in mice

To reliably prevent coprophagia in mice, we utilized functional tail cup devices that were shown to be more effective than the wire floor caging system used by most researchers currently to prevent coprophagia⁴⁰. We constructed both functional tail cup devices to prevent coprophagia and non-functional mock cup devices that do not prevent coprophagia, based on previously published designs (**Figure 3.1B-D**). In the original pilot experiment performed by the designers of the tail cups, mice in both functional tail cup and non-functional mock cups experienced significant weight loss compared to control mice not in cups⁴⁰. However, we did not observe such weight loss in our experiments (**Figure 3.1E**).

3.3: Prevention of coprophagia leads to a loss of anaerobic bacteria in the upper GI tract

We first wanted to ensure we were able to replicate the findings from the original tail cup experiments that coprophagia changed the composition of the microbiota in the upper GI tract⁴⁰. Furthermore, since the original pilot did not have standardized time points collected across all mice, we wanted to know how soon these changes occur in mice after application of cups. We outfitted naïve specific-pathogen free (SPF) C57BL/6 mice with either functional tail cup devices to prevent coprophagia or non-functional mock cup devices that do not prevent coprophagia (**Figure 3.2A**), then housed them in separate sterile cages to prevent sabotage of the device by cage mates.

After 24 hours in their respective devices, luminal content from the jejunum (Figure 3.2B), ileum (Figure 3.2D), and colon (Figure 3.2F) were collected from all mice and then subjected to 16s rRNA-sequencing analysis. We observed a dramatic change in the composition of the apparent microbiota in the small intestinal samples, with a total loss of the obligate anaerobic bacteria seen in the samples of mice with mock cups (Figure 3.2B-F). The change in composition was also reflected in the change in their alpha diversity scores (Figure 3.2C-G). The small intestinal microbiota of the non-coprophagic mice was largely dominated by *Lactobacillus*, with some *Staphylococcus*, and some *Enterococcus faecalis*. Since *Staphylococcus* are generally considered to be a skin commensal microbe, it is possible that this is reflective of the ingestion of skin bacteria through self-grooming habits. Supporting this, their proportion was significantly decreased in ileum samples compared to jejunal samples (Figure 3.2B-D), suggesting these bacteria do not survive very far into the GI tract. Similarly to mice in tail cups, mice in mock cup devices also were mostly dominated by Lactobacillus, but with

relative abundance reaching ~50% at most, rather than the 100% *Lactobacillus* dominated microbiota seen in multiple mice in tail cups. Lactobacilli are commonly associated with the commensal microbiota of the human SI, so their presence in the SI of mice was expected.

Mice given mock cups had large proportions of Lachnospiraceae species in their upper GI tract, as well as Bacteroidales and Ruminococcaceae, contributing to their increased diversity scores in these areas (**Figure 3.2C-E**). These are all obligate anaerobic bacteria, who would not be able to grow in the increased oxygen levels of the SI, and they are not usually found in the healthy human SI⁴². This suggests that these bacteria are not actually engrafting into the SI, and are likely just the result of ingestion of these bacteria from the LI. Despite the dramatic shift seen in the SI microbiota composition, the composition of the LI remained similar between mice in tail cup and mock cup devices. Prevention of coprophagia did not alter the diversity of the LI microbiota (**Figure 3.2G**), with mice in tail cups maintaining a similar taxonomy to coprophagic mice, in the same relative proportions (**Figure 3.2F**). These findings are all in agreement with what the original tail cup designers observed⁴⁰; however these results were seen as early as 24 hours after the application of devices, with the change in microbiota composition in the SI maintained for the duration of time that mice are kept in the cups.

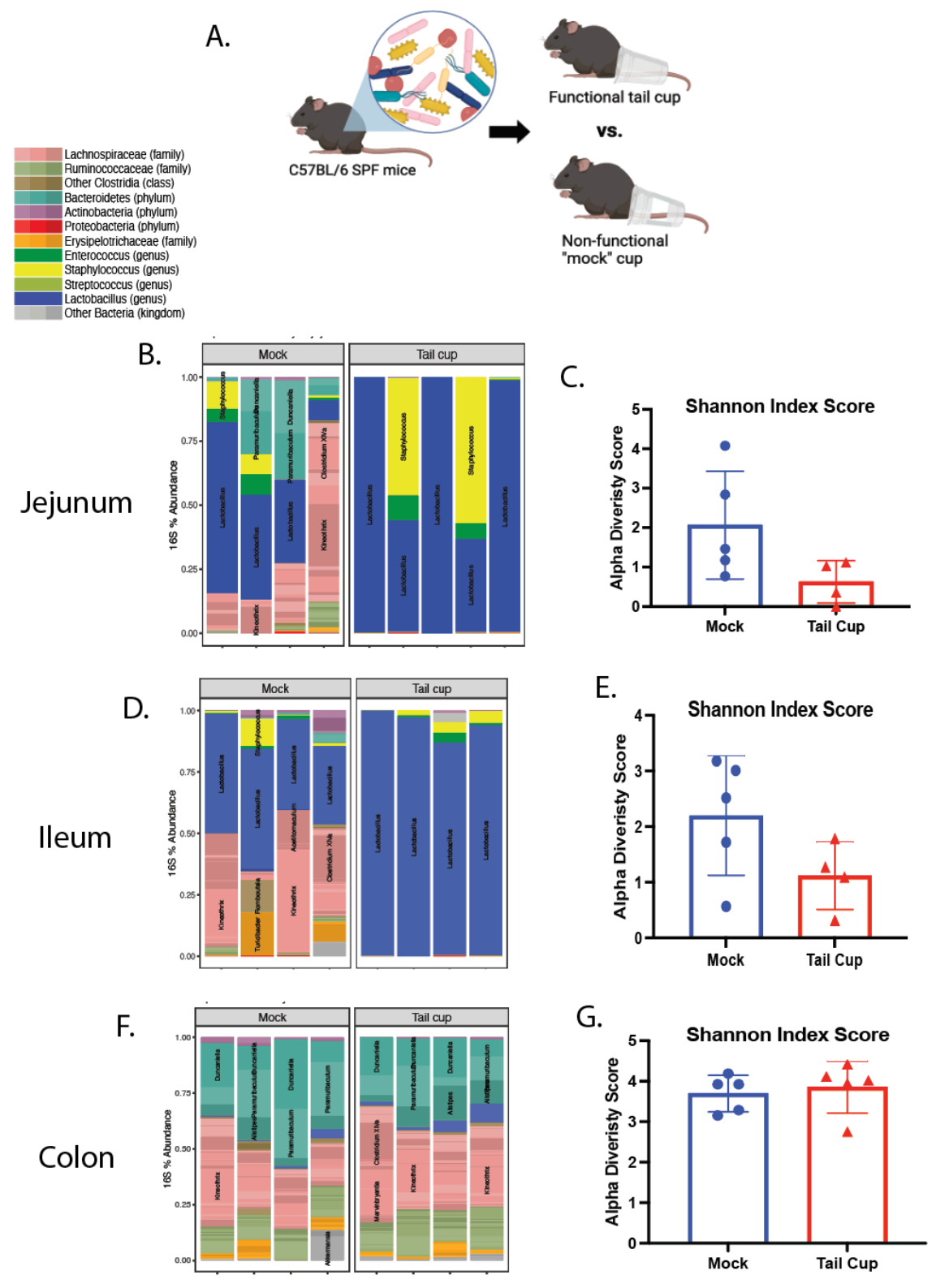


Figure 3.2. Prevention of coprophagia leads to a loss of anaerobic bacteria in the upper GI tract. A. Schematic of experimental set-up. SPF C57BL/6 mice were outfitted with either non-functional cups (Mock cups) or functional tail cups that prevent coprophagia (Tail cups)

Figure 3.2 (continued) for 24 hours. **B.** Microbiome composition and **C.** associated Shannon Index scores in the jejunum, **D-E.** ileum and **F-G.** fecal pellets of each mouse. Each bar represents the relative abundance of bacteria, determined by 16s rRNA sequencing, and colored according to taxonomy. Each symbol represents 1 mouse, blue dots = mice given non-functional mock cups, red triangles = mice given functional tail cups.

3.4 Impact of coprophagia on the microbiome metabolites

We next wanted to characterize how coprophagia influenced the functioning of the microbiome by measuring the microbially modified metabolites throughout the GI tract. We hypothesized that similarly to what was observed with the microbiome composition, the heterogeneity of the metabolomic profile throughout the GI tract would be masked by the reingestion of fecal pellets. Analysis of the relative amounts of short-chain fatty acids in the lumen of the upper GI tract showed that these compounds are mostly concentrated to the LI, with peak concentrations seen in the cecum of mice from both groups (Figure 3.3A-B). These results further support the notion that the anaerobic bacteria seen in the SI of coprophagic mice are not actively colonizing this area, as these are produced by many of those same bacteria 43. Moreover, despite being coprophagic and potentially consuming leftover metabolites from their feces, very few mice from the mock cup group had any detectable SCFAs in their SI (Figure 3.3A-B).

Analysis of the LI of mice in functional tail cup devices showed increased relative concentrations of hexanoate, as well as several other fatty acid derivatives such as 4-methylvalerate and 5-aminovalerate (**Figure 3.3A-B**). The increase in metabolites specific to the LI suggests that while the composition of the LI microbiota appears very similar between mouse groups, their functional outputs are impacted from the lack of coprophagia. In contrast to the fatty acid compounds, the amino acids in the gut were more localized to the upper GI tract

segments, likely from the degradation of dietary compounds⁴⁴. The SI of mice in mock cups had the highest relative concentrations of amino acids overall (**Figure 3.3A-B**). Since amino acids such as glycine and proline can play a critical role in Stickland fermentation by certain *Clostridia* bacteria⁴⁵, we quantified their abundance in the ileal lumen of mice after 2 weeks in the cups. We saw a similar trend again with increased concentrations in the mice with mock cups, but this was not statistically significant (**Figure 3.3C**). This increase in free amino acids in coprophagic mice suggests that ingestion of fecal pellets either increases the degradation of dietary compounds in the SI by bacteria, or it increases the bioavailability of amino acids due to ingestion of degradation products of the LI. Further suggesting that there is a functional shift in the large and small intestinal microbiota during coprophagia, we observed a non-significant increase in succinate in the ileum and propionate in the feces (**Figure 3.3C-D**).

We next wanted to determine how removing coprophagia influenced the modification of bile acid metabolites by the gut microbiota. Bile acids are host-derived compounds involved in digestion that are modified by the gut microbiota²³. The original tail cup group found that mice in tail cups had significantly more conjugated bile acids in their SI than the coprophagic mice, which they attributed to the shift in microbiota composition⁴⁰. Their tail cup mice also showed decreased concentration of total unconjugated bile acids in comparison with mice in mock cups. However, they did not see differences in the concentrations of secondary bile acids (SBAs) between mouse groups, and measurements throughout the GI tract were similar regardless of coprophagic status.

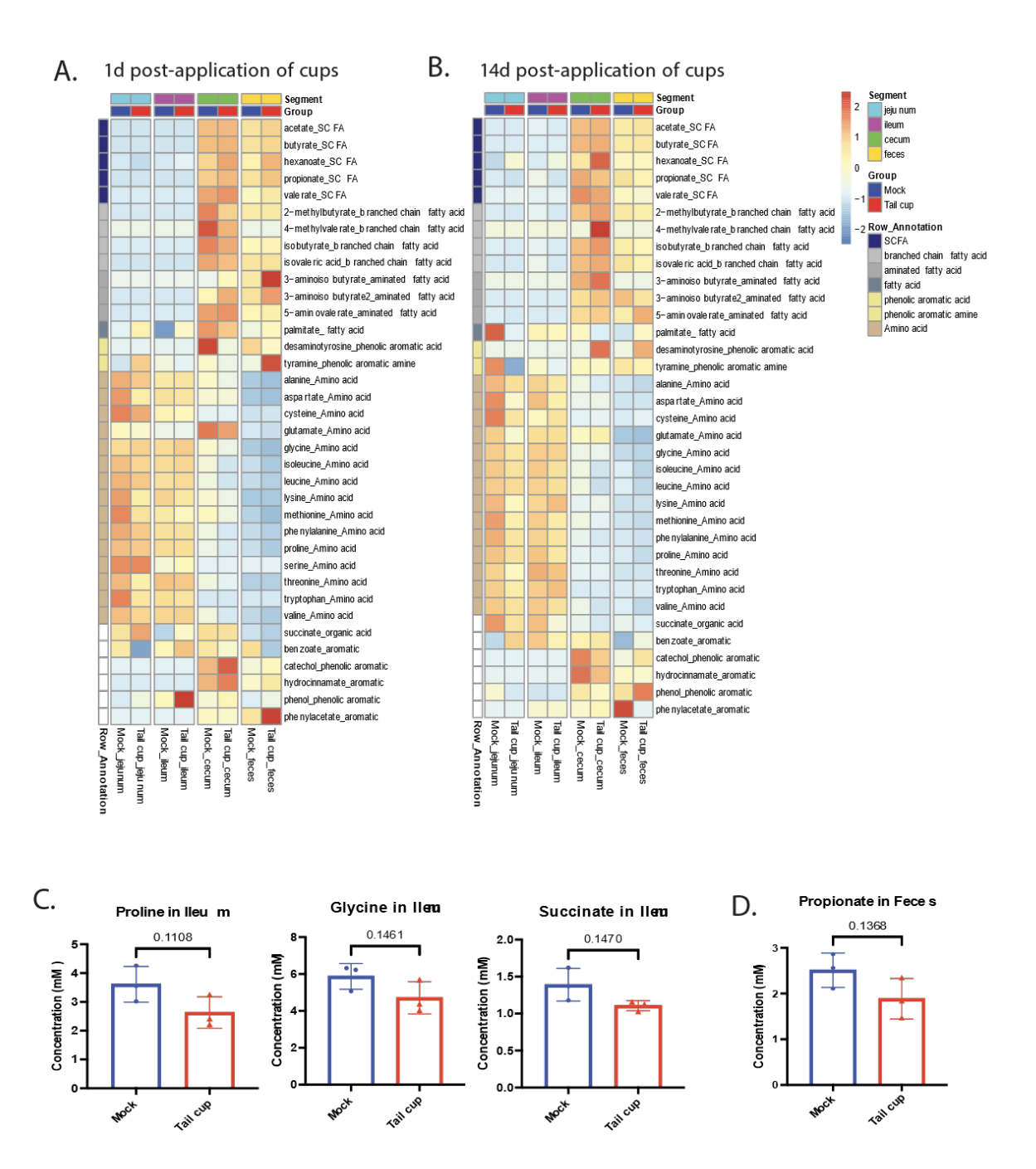


Figure 3.3. Coprophagia increases the concentrations of free amino acids in the small intestine. A. Mice were individually housed and outfitted with functional or non-functional tail cups for 1 day or B. 2 weeks. Heatmap of the normalized median peak value for each listed fatty acid or amino acid. Each tile represents the median value of 3-4 mouse fecal samples, as determined by GC-MS. C. Concentration (mM) of proline, glycine, and succinate in the ileum of mice after 2 weeks in functional tail cups (red triangles) or mock cups (blue dots). Each symbol represents a single mouse. Values are expressed as mean±SD, P values calculated using Student's unpaired t-test.

To analyze the impact of both short- and long-term tail cup use more closely on the bile acid profile of the GI tract, we directly measured 44 different bile acid derivatives in the jejunum, ileum, cecum, and colon of mice (Figure 3.4). Measurement of the conjugated primary bile acids (PBAs), which are synthesized in the liver and secreted directly into the duodenum by the gallbladder²⁴, showed a significant difference in the levels between mouse groups. As early as 24 hours post-cup application, non-coprophagic mice showed a decrease in their glycine-conjugated PBAs (Figure 3.4A-C). However we did not see significant differences in the levels of taurine-conjugated PBAs, contrasting with the findings of Bogatyrev *et al.* who saw no differences in glycine vs. taurine conjugates (Figure 3.4A-C). A similar pattern was observed in the levels of unconjugated PBAs, with significantly less PBAs detected in the jejunum and ileum of non-coprophagic mice after 2 weeks (Figure 3.4B-D).

Finally, we measured the levels of secondary bile acids (SBAs), which are products of modification of PBAs by a small subset of bacteria from the gut microbiota, such as *Clostridium scindens*²⁴. Similar to previous findings, we did not measure significant differences between most of the SBAs of tail cup vs. mock cup mice (**Figure 3.4B-E**). However, we noticed stark differences in the amount of SBAs measured in the SI vs. the LI, with no SBAs measured in the SI of non-coprophagic mice (**Figure 3.4E**). This is more in line with the natural physiology of SBAs, which are known to be modified in the colon. Some coprophagic mice had measurable SBAs in their upper GI tract, which could be from the SBA being in a recently ingested fecal pellet, or from the active deconjugation of PBAs by colonic bacteria that are in transit postingestion.

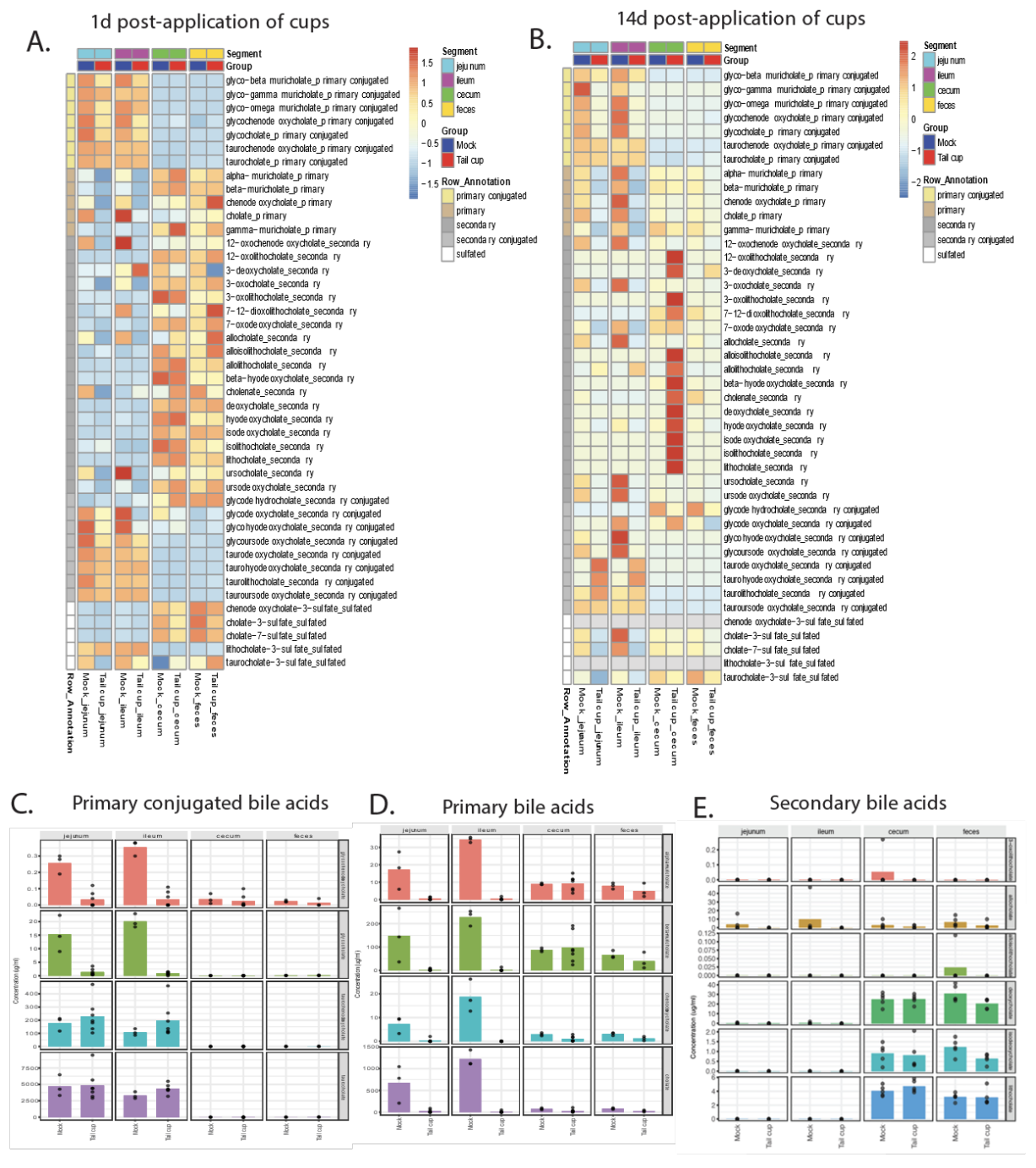


Figure 3.4. Coprophagia increases the abundance of both host and microbially-modified metabolites in the SI. A. Mice were individually housed and outfitted with functional or non-functional tail cups for 1 day or B. 2 weeks. Heatmap of the normalized median peak value for each listed bile acid compound. Each tile represents the median value of 3-4 mouse fecal samples, as determined by LC-MS. C. Concentration (μ g/mL) of primary conjugated bile acids, D. primary bile acids, and secondary bile acids in mice with either functional tail cups or mock cups for 2 weeks. Each symbol represents a single mouse.

3.5: Coprophagia increases activation of the intestinal immune system

We next wanted to know how the shift in the SI microbiota of non-coprophagic mice would impact their intestinal immune system. We hypothesized that the lack of coprophagia would lead to a decrease in the Reg3g expressed, due to the overall reduction in immunostimulatory bacterial molecules encountered by the host epithelium and innate immune cells. Indeed, we found that the expression of Reg3g in the distal ileum of mice in tail cups was significantly reduced compared to mice in mock cups. This reduction could be observed as early as 1 day post-application of tail cups, mirroring the rapid shift seen in the composition of the SI microbiota (Figure 3.5A). The expression of Reg3g in tail cup mice continued to decrease over time, with even less Reg3g mRNA detected in the ileum of mice after 2 weeks, while levels in mock cup mice remained undisturbed (Figure 3.5A).

The bacteria colonizing the gut can have a dramatic effect on the immune tone of the intestine 46,47. Production of Reg3g can be a result of activation of innate immune cells such as CD103+ dendritic cells 22. The decreased expression of Reg3g in tail cup mice suggested that the innate immune system in their SI had a less activated phenotype. We hypothesized that this phenotype would be reflected in the priming of the adaptive immune system, with a shift away from T helper 17 (Th17) cells, towards more regulatory T cells (Tregs). Analysis of T cell populations in the mesenteric lymph nodes of mice after 2 weeks in the tail cups showed a modest reduction in their proportion of Th17 cells compared to mice in mock cups (**Figure 3.5B-C**). While there were no statistically significant differences in their proportions of Tregs, there was a slight decrease in the proportion of Rorgt+ Tregs in mice with tail cups (**Figure 3.5D-F**). These data suggest that the absence of ingestion of the microbiota, microbially-modified

metabolites, and/or bacterial ligands from the LI has functional consequences on the activation of the immune system in the SI.

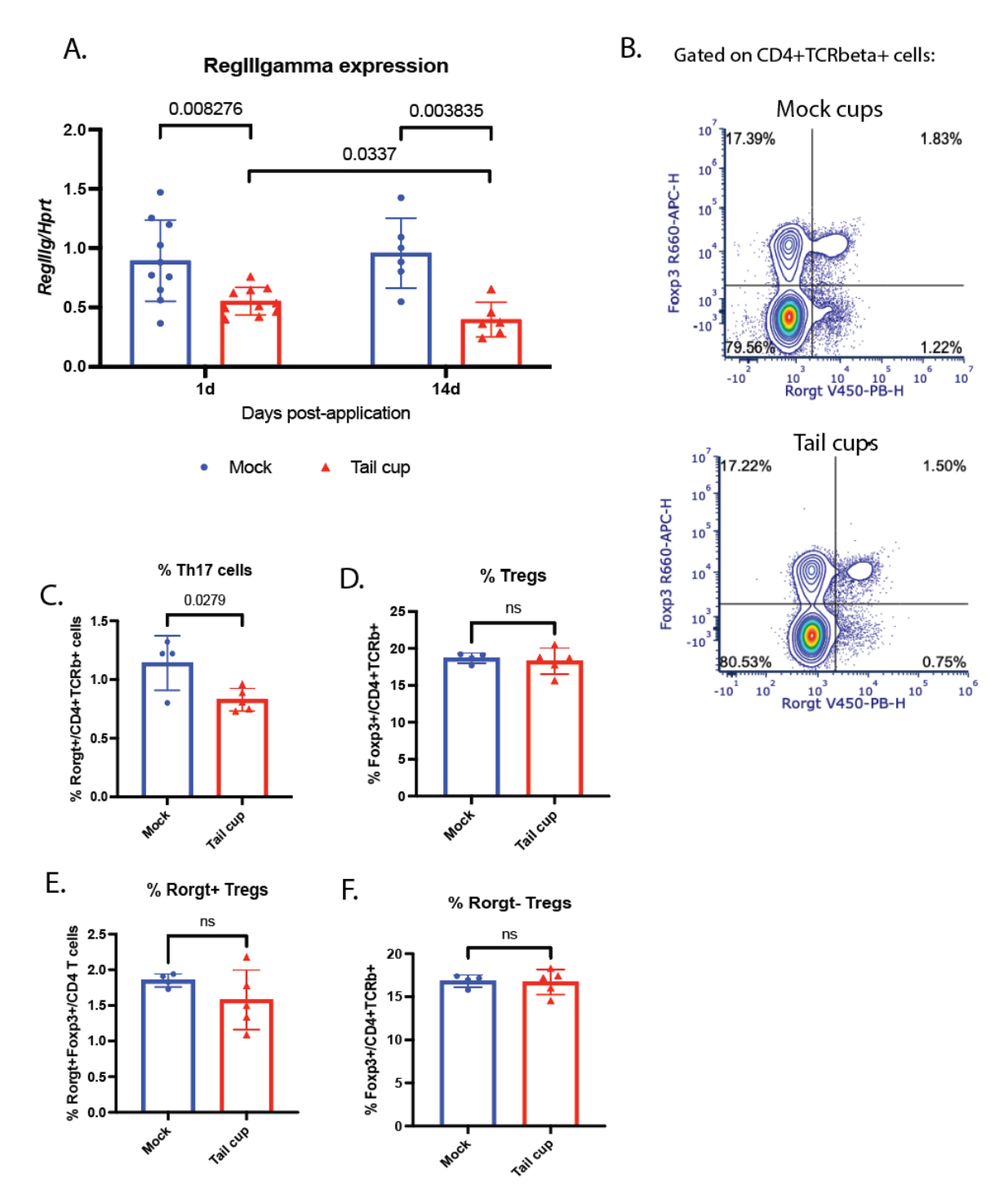


Figure 3.5 Preventing coprophagia in mice leads to a reduction in the stimulation of the intestinal immune system. A. Expression fold change of $Reg3\gamma$ (normalized to Hprt) in the distal ileum of mice after 1 day or 14 days post-application of functional tail cups or

Figure 3.5 (continued) non-functional mock cups. **B.** Example flow cytometry plot of cells from the mesenteric lymph nodes of a mouse that wore a tail cup (top) or non-functional mock cup (bottom) for 14 days. Cells are gated on CD4+TCRbeta+ cells. **C.** Percentage of Rorgt+ Th17 cells, **D.** Foxp3+ Tregs, **E.** Rorgt+Foxp3+ Tregs, and **F.** Rorg-Foxp3+ Tregs out of CD4+TCRbeta+ cells, shown in **B.** Each symbol represents a single mouse. Values are expressed as mean±SD, P values calculated using Student's unpaired t-test, P > 0.05 = ns

3.6 Coprophagia prolongs VRE infection, but is not necessary for colonization of the antibiotic-treated SI

Now that we knew how prevention of coprophagia altered the landscape of the intestinal microbiota and the immune system, we wanted to assess how it impacted the ability for VRE to colonize the SI. Tail cups or non-functional mock cups were applied to SPF C57BL/6 mice, followed by challenge with VRE the next morning (**Figure 3.6A**). Fecal pellets were collected every hour from 4-10 hours post-infection (p.i.) to assess how quickly VRE was able to transit through the gut. We found that coprophagic mice had increased fecal shedding of VRE throughout the first 10 hours p.i. in comparison to non-coprophagic mice (**Figure 3.6B**). Enumeration of VRE in the ileal lumen after 24 hours indicated that VRE was unable to colonize this region at all, regardless of whether coprophagia was inhibited or not (**Figure 3.6C**). This data indicates that microbiota-mediated colonization resistance to VRE is effective in the SI of SPF mice and does not depend on coprophagia.

By 24 hours p.i., all of the non-coprophagic mice in tail cups had cleared VRE from their colon; while 3 out of 5 coprophagic mice were still colonized (**Figure 3.6C**). This difference was reflected in the increased VRE shed in the fecal pellets of mice in mock cups observed in the first few hours post-infection (**Figure 3.6B**), and suggests that coprophagia increased the amount of

VRE being cultured from mice. Moreover, the colonization dynamics of mice in tail cup devices indicated that VRE was not able to engraft in any part of the GI tract of SPF mice, with no culturable VRE found in their ileums or colons after 24 hours (**Figure 3.6C**).

We then compared this to mice who were first treated with ampicillin to deplete their endogenous microbiota, then given tail cups or mock cups followed by challenge with VRE (**Figure 3.6D**). This infection model more closely resembles the dynamics of infection in the hospital, wherein patients undergoing antibiotic treatment become vulnerable to VRE¹.

In striking contrast to our observations in antibiotic-naïve mice, ampicillin-treated mice had dense levels of VRE colonization throughout their GI tract 24 hours p.i., and this was not affected by coprophagia (**Figure 3.6F**). Culturing of fecal pellets taken from mice showed that unlike the non-antibiotic treated mice, there were no observable differences in pathogen burden between tail cup and mock cup mice (**Figure 3.6E**). In ampicillin-naïve mice, coprophagic mice maintained a ~log-fold higher number of VRE CFUs in their feces compared to non-coprophagic mice (**Figure 3.6B**). Pre-treatment of mice with antibiotics, however, led to equal VRE levels in fecal pellets following infection (**Figure 3.6E-F**). The quantity of VRE CFUs in the feces of ampicillin-treated mice increased over the first 10 hours of infection, rising to 10^7 CFUs/mg of feces (**Figure 3.6F**), unlike the SPF mice which had the largest quantifiable amount of 10^2 - 10^3 at 4 hours p.i. (**Figure 3.6B**).

Mice in both functional and mock cups exhibited the same VRE engraftment levels, starting with $\sim 10^3$ CFUs in the duodenum and increasing as the GI tract descends, reaching the highest levels in the colon (**Figure 3.6F**). The mice in mock cups displayed more heterogeneity in their SI levels of VRE, similar to our observations in the fecal levels of the antibiotic-naïve mock cup's group (**Figure 3.6C, 3.6F**). Regardless of coprophagia though, ampicillin-treated

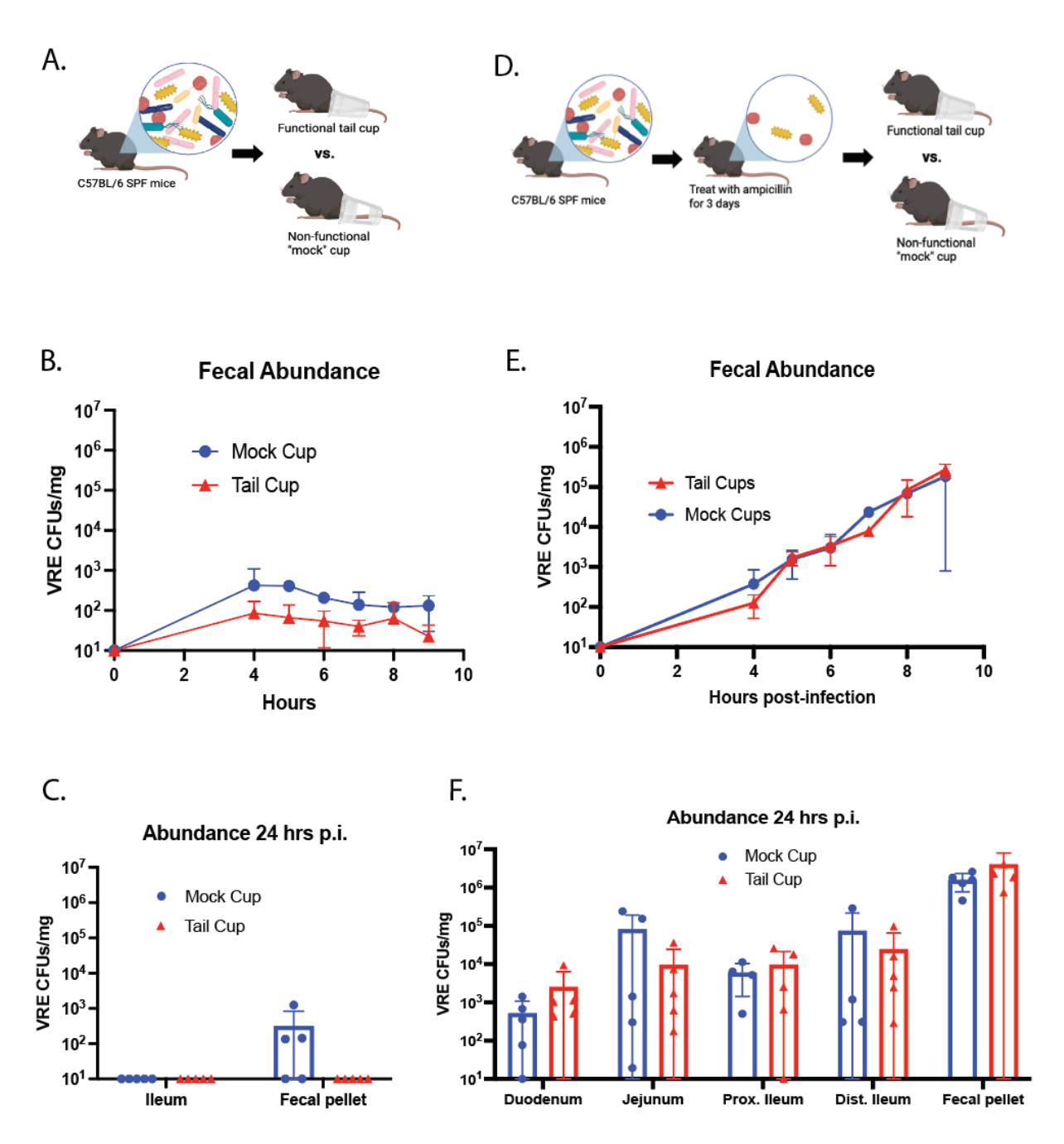


Figure 3.6. Coprophagia prolongs infection with VRE, but is not required to colonize the antibiotic-treated SI. A. Diagram of experimental design. Mice were outfitted with tail cups or mock cups, followed by challenge with VRE the next morning. **B-C.** Abundance of VRE (CFUs/mg) 4-24 hours post-infection of mice outfitted with mock cups (blue circle) or tail cups that prevent coprophagia (red triangles). **D.** Diagram of experimental design. Mice were given ampicillin (0.5g/L) in their drinking water for 3 days prior to application of cups and challenge with VRE. **E-F.** Abundance of VRE (CFUs/mg) 4-24 hours post-infection. Each symbol in **B.** and **E.** represents the average of 4-5 mice; each symbol in **C.** and **F.** represents a single mouse.

mice both had high levels of VRE colonization in their gut. These findings suggest that coprophagia enables VRE reacquisition, potentially making it appear as though mice that are resistant to VRE are colonized. However, VRE colonization of the SI does not depend on coprophagia and thus represents a distinct niche in the gut that is exploited by VRE following antibiotic-induced dysbiosis.

3.7 Prevention of coprophagia enables faster clearance of VRE in the SI

Now that we knew that VRE was capable of engrafting into the SI, we next wanted to characterize the dynamics of recovery from VRE in the SI vs. LI. We treated mice with a short round of ampicillin, then outfitted them with either tail cups or mock cups followed by challenge with VRE (Figure 3.7A). As quickly as 3 days post-infection (p.i.), mice wearing tail cups showed differences compared to mice wearing mock cups in the VRE levels of their SI. Half of the mice in tail cups had no quantifiable VRE in their duodenum by day 3 p.i., and all of them had cleared VRE from their duodenum by day 10 p.i. (Figure 3.7B). In contrast, half of the coprophagic mice in mock cups still had quantifiable VRE in their duodenum at day 10 p.i. (Figure 3.7B). We observed a similar trend in VRE colonization kinetics of the distal ileum, with near total clearance of VRE in the ileum of tail cup mice by day 10 p.i.. This is in comparison to the only ~33% of mice in mock cups that showed clearance by the same timepoint (Figure 3.7C).

The colonization dynamics of the colon indicated slower recovery in this niche compared to the SI, though non-coprophagic mice still showed reduced VRE levels sooner than coprophagic mice (**Figure 3.7D**). By 2 weeks p.i., mice in tail cups had significantly less VRE

CFUs in their fecal pellets compared to mice in mock cups. In all mice tested, VRE was cleared sooner the higher the location in the GI tract they were colonizing, remaining in the large intestine for the longest duration of time in all mice tested (**Figure 3.7B-D**). The quicker clearance of VRE in the SI of mice in tail cups implies that coprophagia of VRE colonizing the LI leads to quantifiable VRE in the upper parts of the GI tract, which is supported by the finding that VRE densely colonized the LI of non-coprophagic mice up to 14 days p.i. (**Figure 3.7D**).

These findings suggests that elimination of VRE from the SI is independent of the LI, with de-colonization of the SI preceding the LI. This trend was observed in both groups of mice but occurred more quickly in mice outfitted with tail cups (Figure 3.7B-D). We hypothesized that recovery of VRE in the SI was mediated by the recovery of the host immune system, so we measured transcription of Reg3g in the distal ileum of mice. We found that the timing of recovery of Reg3g expression in non-coprophagic tail cup mice mirrored the timing of VRE clearance of their ileum (Figure 3.7E), suggesting that this lectin was involved in elimination of VRE in this area. Tail cup mice displayed an increase in their Reg3g expression at day 10, though the overall amount of Reg3g they expressed was still lower than the mice in mock cups (Figure 3.7E). Compared to mice with tail cups, mice in mock cups also showed quicker recovery of their Reg3g expression, with a significant increase in expression by day 7 p.i. This is in line with our findings in naïve, non-antibiotic treated mice, where the prevention of coprophagia alone decreased the transcription of Reg3g in their SI (Figure 3.5A).

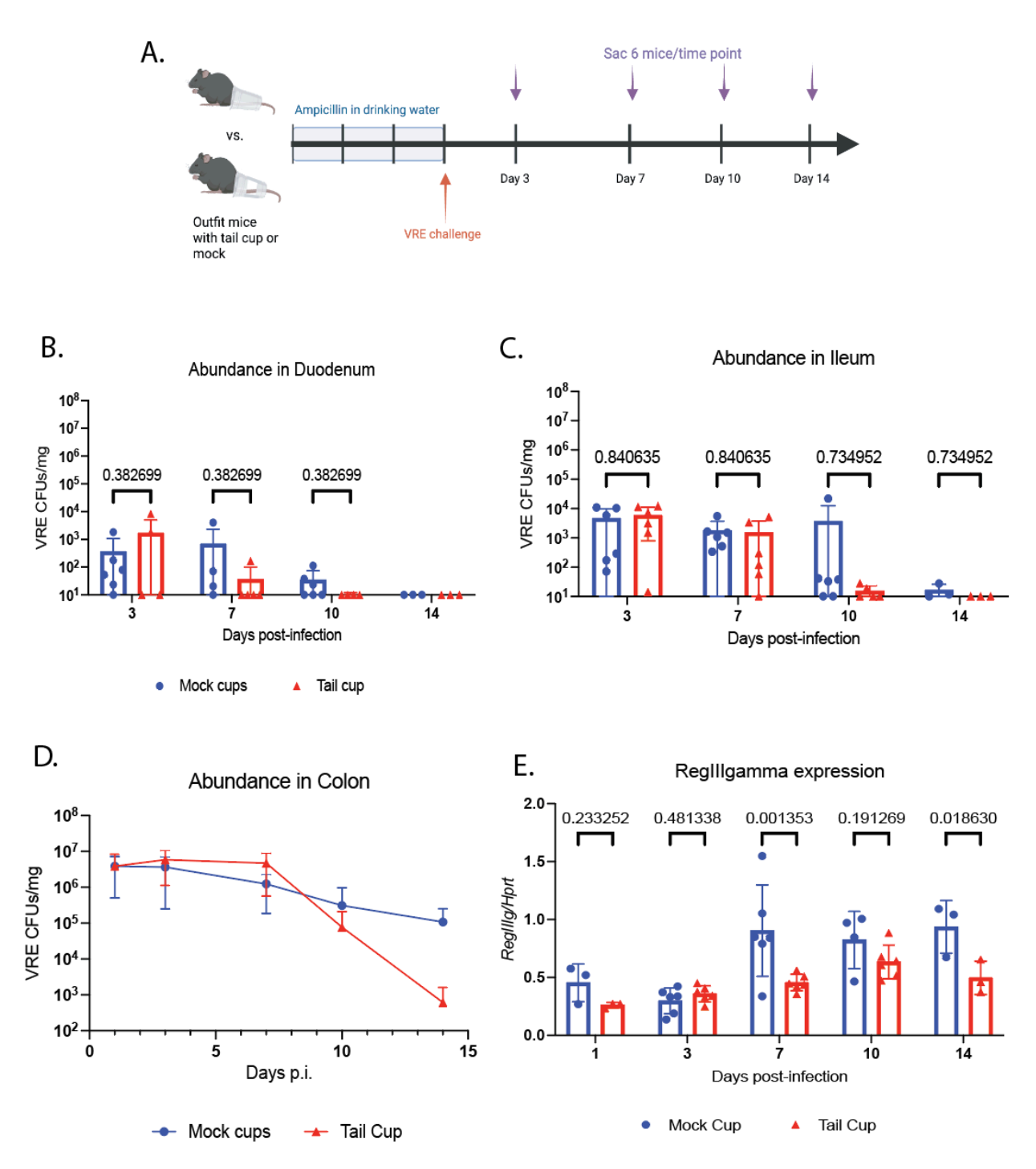


Figure 3.7 Recovery of Reg3g expression after ampicillin-treatment in non-coprophagic mice is sufficient to clear VRE from the small intestine and reduce VRE in the colon. A. Experimental design and timeline. Mice were given tail cups or mock cups and then given ampicillin treatment for 3 days, followed by challenge with VRE. B. Abundance of VRE (CFUs/mg) in the duodenum, C. ileum and D. fecal pellets of mice outfitted with tail cups to prevent coprophagy (red triangles) or mock cups (blue circles). Each symbol in all plots

Figure 3.7 (continued) besides **D.** represents 1 mouse. **E.** Host expression in the distal ileum of *Reg3g* normalized to *Hprt*. Values are expressed as mean±SD, P values calculated using Student's unpaired t-test.

3.8: Enterococcus faecium colonizes the SI epithelium in small clusters

The findings regarding the dynamics of VRE colonization in the gut indicated that the SI was a distinct niche colonized by VRE during its domination of the antibiotic-treated gut.

Maintaining stable colonization of the SI is not a simple task for bacteria though—beyond tolerance of increased oxygen, bacteria must withstand the constant flow of dietary- and host-derived compounds that constantly move through the gut. Previous research into the related species *Enterococcus faecalis*, showed that these bacteria could form microcolonies along the (coprophagic) mouse epithelium, in the duodenum, ileum, and colon⁴⁸. Furthermore, *E. faecium* is known to have genes involved in host-adhesion and biofilm formation⁶. This led us to speculate that *E. faecium* could directly engraft onto the SI epithelium, forming discrete populations in the SI niche.

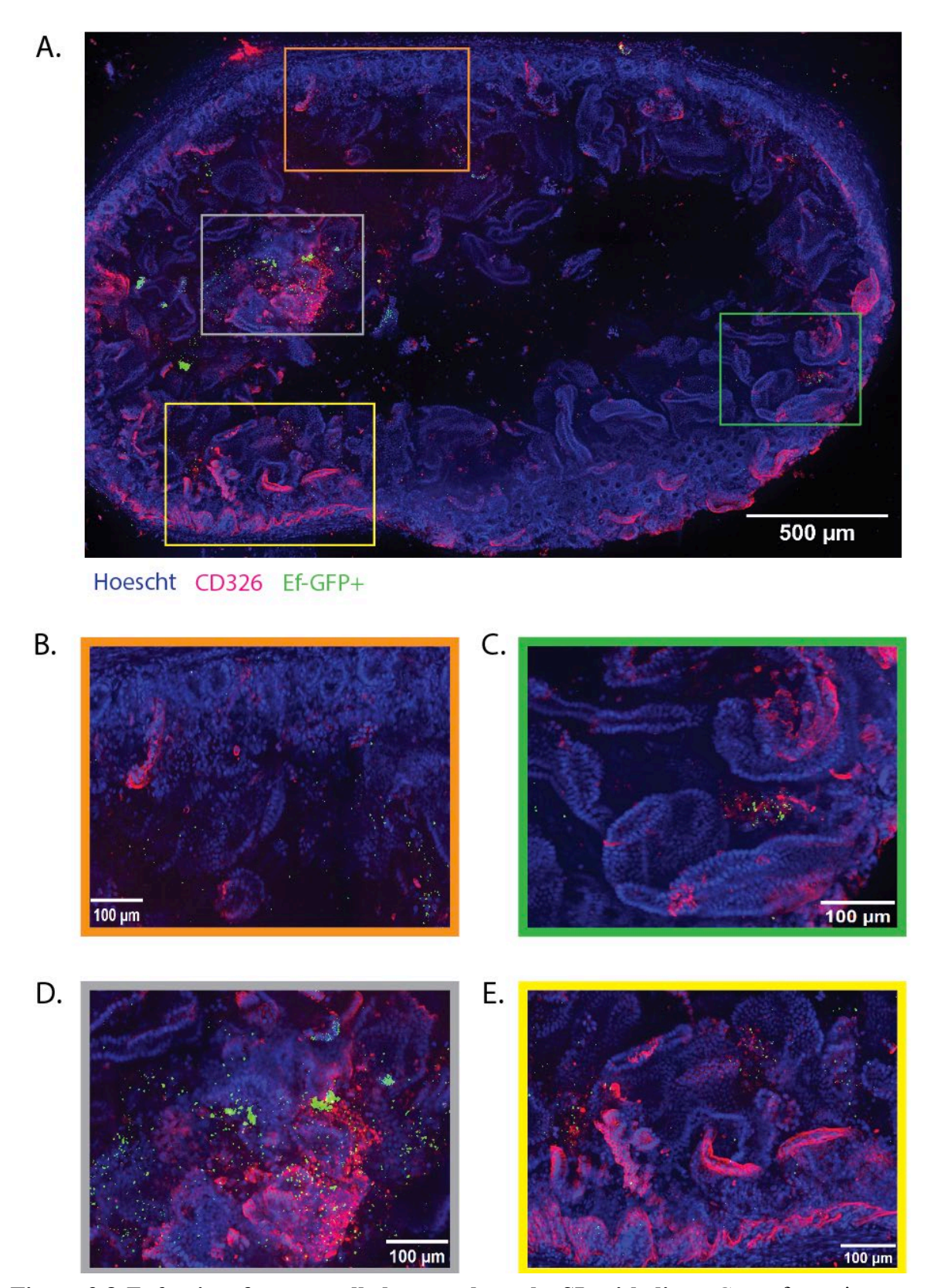


Figure 3.8 *E. faecium* **forms small clusters along the SI epithelium.** Germ-free mice were associated with GFP+ *Enterococcus faecium* strain com15 then outfitted with a functional

Figure 3.8 (continued) tail cup. Image of a representative sample from the distal ileum, 300 um max-projection Z-stack taken at 20x on a SoRa Marianas Spinning Disk Confocal microscope. **A.** Stitched together tiles showing the entire segment of ileum imaged. **B-E**. Zoomed in square insets of bacterial clusters.

To test this hypothesis, we utilized a green-fluorescent protein expressing strain of
Enterococcus faecium (Ef-GFP+) to directly visualize associations of the bacterium with the
mouse intestinal epithelium. We applied either tail cup or mock cup devices to germ-free mice,
followed by association with Ef-GFP+. After 2 weeks, we imaged the distal ileums and colons of
mice using a spinning disc confocal microscope. We found that throughout the gut, small
populations of Ef-GFP+ bacteria formed clusters amongst the epithelial cells (Figure 3.8). We
observed these Ef-GFP+ clusters in mice from both cup groups, suggesting that these clusters
persist in the SI without the need for re-seeding from the LI (Figure 3.9A-B). Moreover, we
found the Ef-GFP+ clusters in the colon of both coprophagic and non-coprophagic mice,
suggesting that this colonization phenotype was not specific to the LI (Figure 3.9C-D). The
formations of Ef-GFP+ in the SI were similar to those formed by E. faecalis, but the clusters
were smaller and less dense overall⁴⁹. Quantification of the size of the Ef-GFP+ clusters of noncoprophagic mice indicated that these populations were larger in the ileum than the colon,
despite there being a smaller density of bacteria in this niche (Figure 3.9E-F).

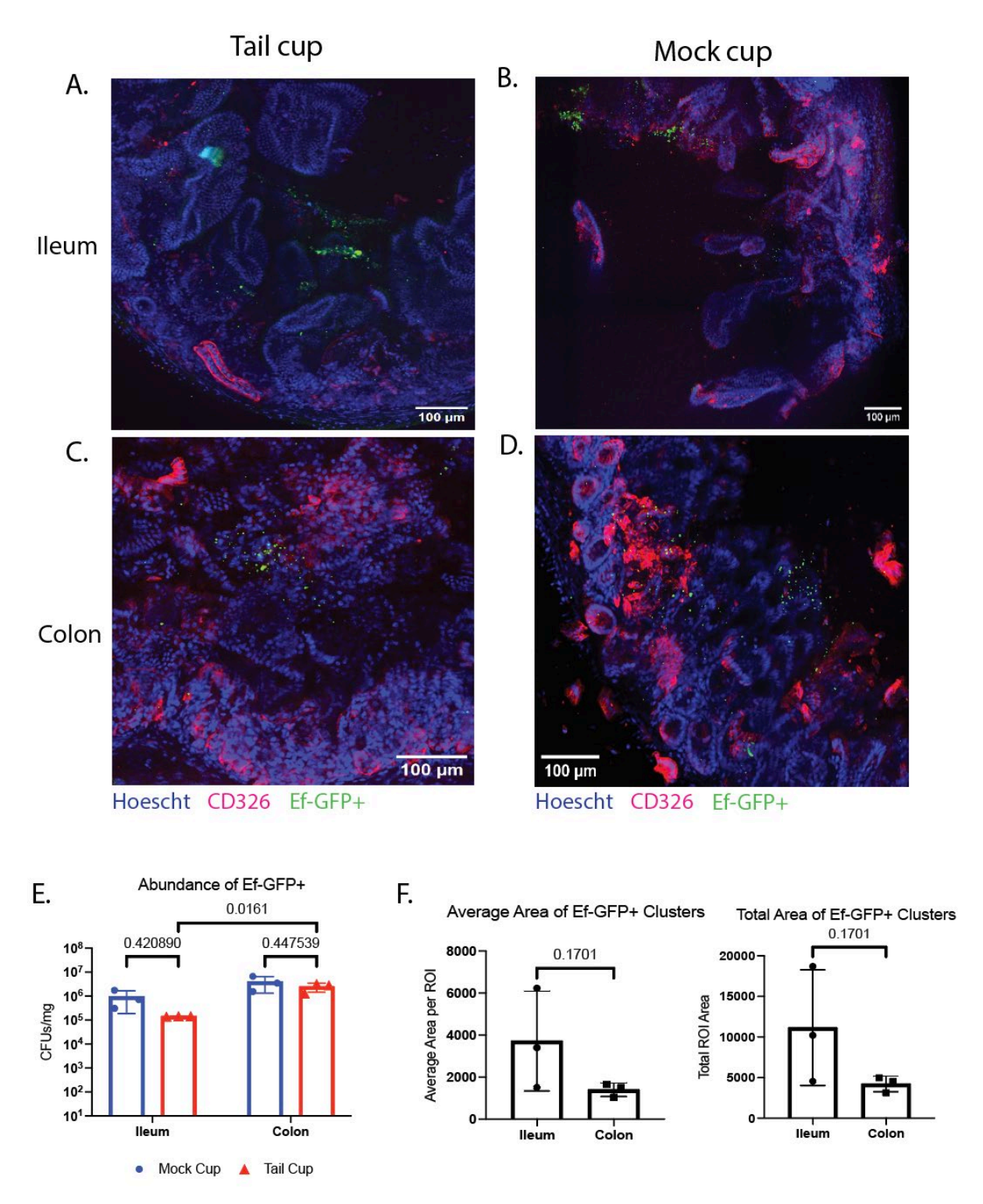


Figure 3.9 Non-coprophagic mice have increased Ef-GFP+ clusters in their ileum. Germ-free mice were associated with GFP+ *Enterococcus faecium* strain com15 then outfitted with a functional tail cup or mock cup. Representative sample images of the **A.** ileum of a tail cup vs. **B.** mock cup mouse, as well as the **C.** colon of the tail cup and

Figure 3.9 (continued) D. mock cup mice. **E.** Quantification of Ef-GFP+ CFUs from the ileum vs. colon of mice from both groups. **F.** Average (right) and total (left) area of the Ef-GFP+ clusters in the ileum vs. colon of mice wearing tail cups. Images are all 300 um max-projection Z-stack taken at 20x on a SoRa Marianas Spinning Disk Confocal microscope.

3.9 Summary of results

We determined that there are distinct colonization and recovery dynamics to VRE infection in the different regions of the GI tract, and that these dynamics have been obscured in past experimental models due to mouse coprophagia. We found that removal of VRE from the SI preceded clearance from the LI, suggesting that this niche is separate from the LI niche, but likely contributes to overall fecal shedding. The prevention of coprophagia dramatically altered the composition and metabolomic functioning of the microbiota, leading to a decrease in stimulation of the intestinal immune system. Though the SI immune system was less activated in non-coprophagic mice, the prevention of pathogen recycling enabled the decoupling of this phenomenon from the dynamics of the Reg3g production recovery on VRE clearance, indicating that this level was still sufficient to eliminate VRE from the SI.

CHAPTER 4: Commensal bacteria shield the gut microbiota from ampicillininduced dysbiosis and preserve colonization resistance against antibiotic-resistant pathobionts

4.1 Introduction

The collateral damage done to the commensal gut microbiota after antibiotic treatment has been a widely recognized issue in the field of infectious diseases for decades now, with the threat of infection with antibiotic-resistant pathogens continuing to escalate over time⁵⁰. The endogenous commensal gut microbiota are critical for providing colonization resistance to pathogens that contaminate hospitals such as vancomycin-resistant *Enterococcus* (VRE), carbapenem-resistant *Enterobacteriaceae* and *Clostridioides difficile*⁹. The vulnerability that patients are left with after primary treatment with antibiotics remains an ongoing and urgent public health threat.

Our previous investigations into the microbiota of our mouse colony indicated the potential for antibiotic-resistant microbiota to be leveraged for the assembly of protective bacterial consortia. We found that this mouse colony maintained a diverse microbiota during antibiotic treatment, and this phenotype could be transferred to other ampicillin-treated mice through fecal microbiota transplant (FMT)¹⁷. Further investigations into this microbiota led to the isolation of a 4-member bacterial consortium that could degrade ampicillin and impart colonization resistance to VRE¹⁶. However, these mice had experienced prolonged exposure to beta-lactam antibiotics for the past 2 decades, rendering it unclear as to whether this phenotype could occur in healthy microbiomes with no prior treatment history. While antibiotic usage

increases evolutionary pressure^{51,52}, it is not a requirement for the development of these functions, and antibiotic-resistance can be found in the gut microbiota of people without any prior history of exposure⁵³. The naturally occurring variations in susceptibility of patients to antibiotics suggests that there are many healthy individuals with antibiotic-resistant microbiomes^{54,55}. Further investigations into the identification of antibiotic-resistant bacterial consortia derived from healthy, non-antibiotic treated microbiota are therefore warranted.

Studies diving into the unique qualities of the microbiota of individual mouse colonies from commercial vendors has yielded many insights for researchers, such as the discovery of segmented-filamentous bacteria in mice from Taconic, which induce a robust Th17 phenotype in the SI⁵⁶. We therefore utilized commercially available mice to assess antibiotic resistance potential in healthy microbiota unexposed to antibiotics⁵⁷. We tested mice from different colonies for their susceptibility to ampicillin-induced dysbiosis and examined their colonization resistance to VRE. We found that 1 out of 7 colonies tested was resistant to ampicillin, and we identified 3 beta-lactamase producing bacteria from the gut microbiota of this colony that could confer ampicillin-resistance to a different ampicillin-sensitive microbiota. These studies provide a framework for further investigations into the use of commensal bacterial consortia to shield the endogenous microbiota from antibiotic-mediated disruption.

4.2 One out of the seven different mouse microbiota tested was resistant to ampicillin-induced dysbiosis

To investigate the potential for ampicillin-resistance in healthy, antibiotic-naive microbiota, we made use of commercially available in-bred C57BL/6 mouse colonies from two different vendors (Jackson Laboratory and Charles River Laboratories). These mice are carefully reared to be disease-free, have no reported history of antibiotic exposure, and generally have stable, complex microbiota that are consistent across all mice within the breeding colony group⁵⁷. We selected 7 different mouse breeding colony groups across 3 geographically distinct sites (Figure 4.1A, Table 4.1) and tested their microbiome's susceptibility to ampicillinmediated dysbiosis. We determined the fecal microbiota composition of 4-5 individually-housed mice from each breeding colony group by 16s rRNA-sequence analysis, prior to ampicillin treatment (Figure 4.1B-C) and after 3 days of ampicillin in their drinking water (Figure 4.1B-**D**). Principal Coordinate Analysis (PCoA) of Bray-Curtis dissimilarity scores showed clustering along PCoA1 of microbiome samples by the commercial vendor the mice originated from, regardless of antibiotic treatment status or geographic site (Figure 4.1B). Most microbiome samples from ampicillin-treated mice separated away from their naïve counterpart samples along PCoA2, except for those from mouse group H47, a breeding colony group reared by Charles River Laboratories (CR). All fecal microbiome samples of mice from this group clustered tightly together, with their taxonomy remaining relatively unchanged after the introduction of antibiotics (**Figure 4.1B-D**). This is in contrast to the 6 other mouse microbiota groups, which all displayed a rapid shift in composition after ampicillin treatment, with a dramatic loss of obligate anaerobic bacterial species belonging to the Bacteroidota phylum and Lachnospiraceae family, key

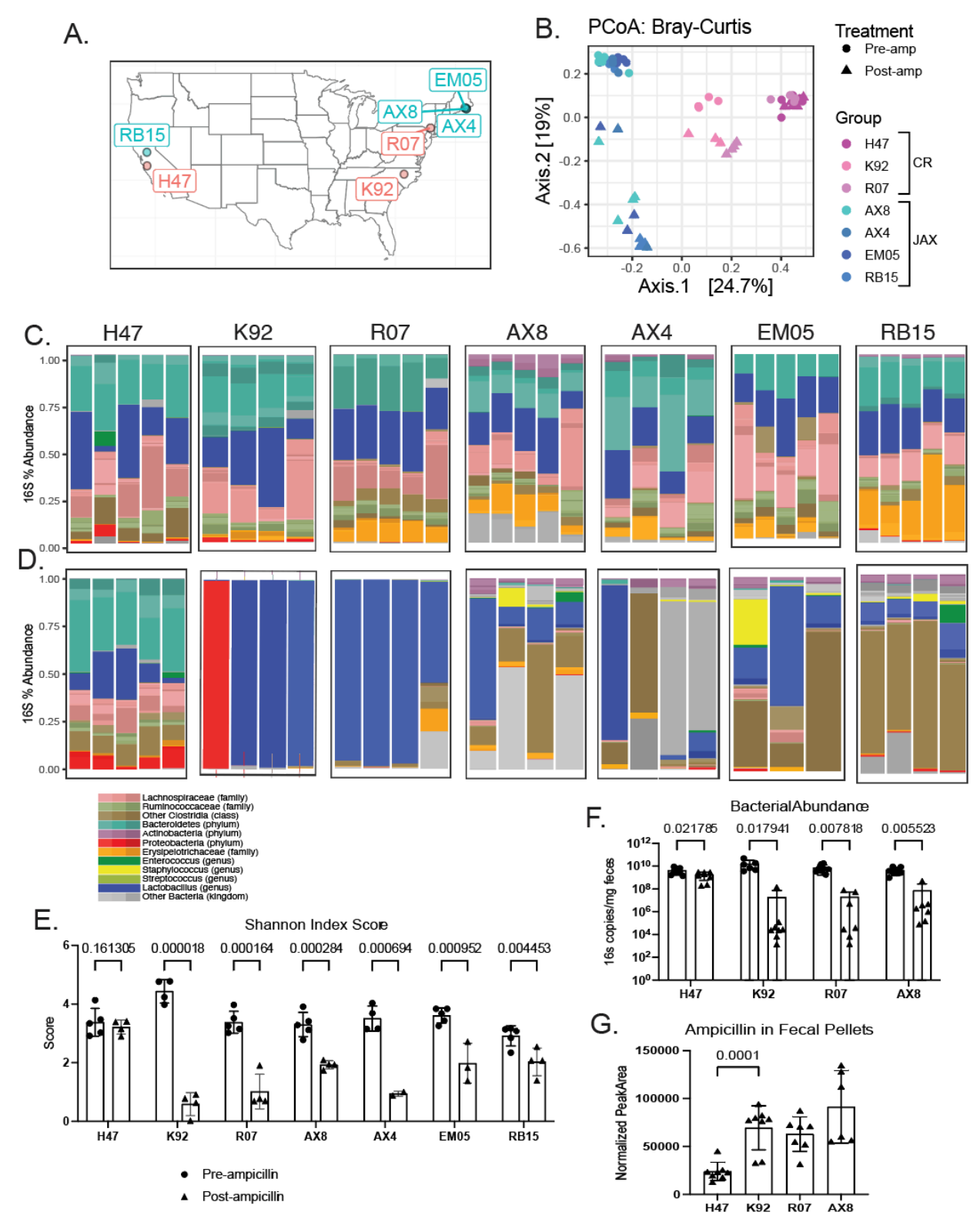


Figure 4.1 One out of the seven different microbiota tested were resistant to ampicillininduced dysbiosis. A. Map of locations of C57BL/6 mouse groups tested from two

Figure 4.1 (continued) commercial vendors, Jackson Labs (blue) and Charles-River Labs (pink). **B.** Principal coordinate analysis of the Bray-Curtis dissimilarity between mouse microbiomes pre-ampicillin treatment (circles) and after 3 days of treatment with 0.5g/L of ampicillin in their drinking water (triangles). Each symbol is colored by group and represents an individual mouse fecal microbiome, n = 4-5. **C.** Taxonomic composition of the fecal microbiomes plotted in **B.** from each mouse group, before and **D.** after the start of ampicillin treatment. Each bar represents the individual fecal microbiome of a single-housed mouse. **E.** Shannon index scores of the fecal microbiomes plotted in **B-D. F.** Absolute abundance of bacteria in feces, as determined by qPCR for 16s rRNA copies. **G.** Ampicillin in the fecal pellets of mice during treatment with ampicillin, as determined by LC-MS. Each dot represents an individual mouse fecal pellet, raw values normalized to raw peak area values from each mouse's feces pre-ampicillin treatment. **E-G.** Each symbol represents a single fecal microbiome, pre-ampicillin treatment (circles) or after 3 days of treatment with ampicillin (triangles). P-values calculated using unpaired t-test.

Mouse group	Commercial vendor	Location of breeding colony
H47	Charles River Labs	Hollister, CA, USA
K92	Charles River Labs	Kingston, NY, USA
R07	Charles River Labs	Raleigh, NC, USA
AX8	Jackson Lab	Bar Harbor, ME, USA
AX4	Jackson Lab	Bar Harbor, ME, USA
EM05	Jackson Lab	Ellsworth, ME, USA
RB15	Jackson Lab	Sacramento, CA, USA

Table 4.1. Table of mouse groups and their locations. Mouse groups used for these experiments, with the commercial mouse vendor that bred the mouse group, and the location of the breeding facility the mice were born in. Mouse group names correspond to the individual room that the breeding colony was kept in.

members of a healthy microbiome⁵⁸. The residual microbiota from these mice varied dramatically between groups, but also, to a lesser extent, between mice from the same group (**Figure 4.1D**). The differences in the microbiota of mice from the same group after ampicillin highlight the vast possible trajectories the microbiota can take after perturbation. Mice from the

ampicillin-susceptible CR colonies, R07 and K92, were prone to domination by a single taxa (*Lactobacillus* or *Proteus*) (**Figure 4.1D**). This contrasts with mice from Jax colonies, who retained a higher number of different species, but at much lower proportions than the non-ampicillin treated samples (**Figure 4.1C-E**). The microbiome samples from group R07, also from CR, clustered with the H47 samples before exposure to ampicillin (**Figure 4.1B**), highlighting how similar the microbiomes were in composition before the introduction of ampicillin (**Figure 4.1C-D**).

Further suggesting that mice from group H47 harbored a gut microbiome that was resistant to ampicillin, they retained their same level of fecal bacterial diversity (Figure 4.2E) and abundance (Figure 4.2F) after the introduction of ampicillin. Resistance to ampicillin in anaerobic bacteria can be conferred by a variety of mechanisms, such as production of betalactamases that hydrolyze the antibiotic, modification of penicillin binding proteins, and blocking penetration of the antibiotic^{36,59}. We hypothesized that the H47 mice contained resistant bacterial strains in their gut microbiota that were inactivating the ampicillin, protecting the susceptible bacteria from destruction⁶⁰. We therefore measured by LC-MS the amount of ampicillin present in their feces and compared it to the mice tested from other groups to determine if the ampicillin from the drinking water was present in the gut of H47 mice (Figure **4.2G**). We found that there was significantly less ampicillin present in their feces compared to mice from the other groups tested, despite all mice receiving treatment with ampicillin water. These results support the notion that resistant bacteria from the microbiota of H47 mice are depleting ampicillin in the intestinal lumen, shielding the sensitive bacteria and maintaining community stability.

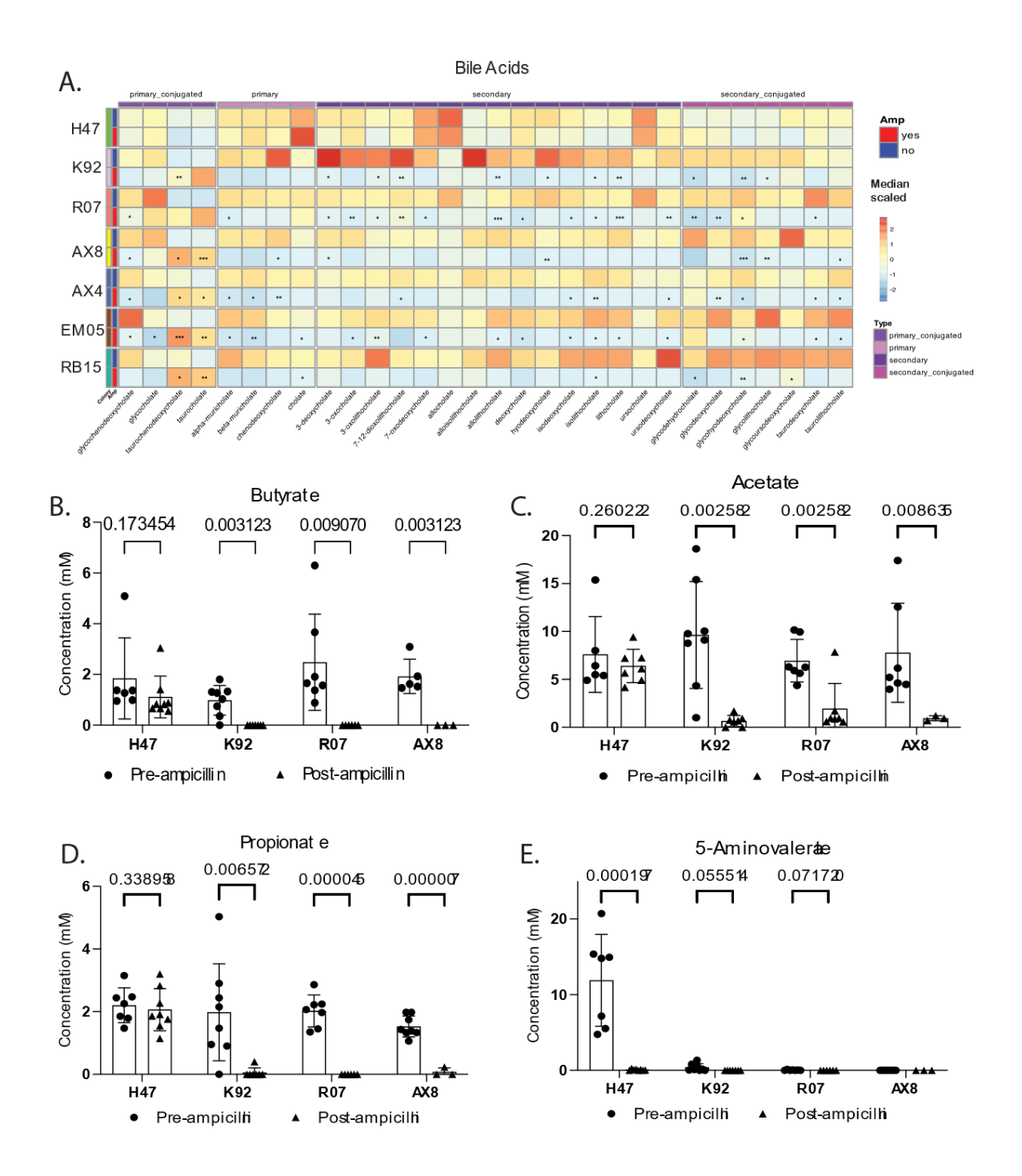


Figure 4.2 Ampicillin-resistant microbiota retain production of most bile acid and short chain fatty acid metabolite compounds after perturbation with ampicillin. A. Heatmap of the normalized median peak value for each listed bile acid compound, as determined by LC-MS. Each tile represents the median value of 3-4 mouse fecal samples, scaled by compound. P-values * < 0.05, unpaired t-test of median values of each mouse group before and after starting ampicillin treatment (0.5g/L) in the drinking water. B. Concentration (mM) of butyrate, C. acetate, D. propionate, and E. 5-aminovalerate in the

Figure 4.2 (continued) fecal pellets of mice pre-ampicillin treatment (circles) and after 3 days of ampicillin treatment (triangles). Each symbol represents a single individually-housed mouse. P-values calculated using unpaired t-test.

4.3: Ampicillin-resistant microbiota retain production of most bile acid and short chain fatty acid metabolite compounds after perturbation with ampicillin.

To further assess the levels of dysbiosis in the microbiota of the different mouse groups, we examined their microbially-modified metabolite levels. Fecal pellets taken from mice before and after the introduction of antibiotics were analyzed for their relative amounts of bile acids, one of the primary groups of metabolic compounds modified by bacteria in the intestine²⁴ (Figure 4.2A). We found that ampicillin treatment led to a reduction in primary, secondary, and modified secondary bile acids from mice harboring ampicillin-susceptible microbiota. This likely reflects the loss of the smaller population of bacterial species within healthy microbiota that modify bile acids⁶¹, and is consistent with the broad reduction in anaerobic bacterial species observed in susceptible mouse groups after ampicillin treatment (Figure 4.1). In contrast, the overall bile acid profile of fecal samples obtained from H47 mice remained consistent after ampicillin exposure, with non-significant reductions in some secondary bile acids, like lithocholate and its derivates such as 3-oxolithocholate and isolithocholate (Figure 4.2A). These findings are consistent with our observations that the colony H47 is resistance to ampicillininduced dysbiosis, as they are the only group that maintained their bile acid profile during ampicillin treatment.

Measurement of short-chain fatty acid concentrations in the feces of mice revealed a similar trend, with H47 mice maintaining consistent production of butyrate, propionate, and acetate during treatment with ampicillin (**Figure 4.2B-D**). A microbially modified compound that was unique to H47 mice in comparison to the other microbiota groups tested was 5-aminovalerate (5-AV), which was then markedly reduced by ampicillin treatment (**Figure 4.2E**). 5-AV is produced by certain bacteria in the gut microbiome such as, *Clostridium sporogenes*, from the metabolism of proline by Stickland fermentation⁶². The loss of this metabolite is indicative of the functional changes induced in the gut microbiota by treatment with ampicillin. These results suggest that while there were not dramatic shifts in taxonomic structure, the ampicillin treatment was not entirely without impact on the gut microbiota of H47 mice. Altogether though, the consistency in overall metabolomic profile of the H47 mice during treatment implies that their gut microbiota was resistant to ampicillin.

4.4: Ampicillin-resistant bacteria isolated from the H47 microbiome

Reduced concentrations of ampicillin in fecal samples from H47 mice (**Figure 4.1G**) suggested that there were commensal bacteria in their microbiota degrading the ampicillin⁶³. In our previously isolated consortium of bacteria from an ampicillin-resistant microbiota (ARM), the beta-lactamase producing *Bacteroidales* members (*Bacteroides sartorii*_{ARM} and *Parabacteroides distasonis*_{ARM}) provided protection to the ampicillin-sensitive lantibiotic-producing *Blautia* member when colonizing ampicillin-treated mice¹⁷. We reasoned that the

antibiotic-resistance phenotype of the H47 microbiota could similarly be traced to a smaller subset of resistant bacteria. This notion was supported by the earlier observation that the H47 microbiome samples were similar in overall taxonomic composition to microbiome samples taken from the ampicillin-sensitive R07 mice (CR) before ampicillin treatment (**Figure 4.1B-C**). To determine which bacteria were uniquely enriched in the ampicillin-resistant H47 microbiota, we performed metagenomic sequencing on fecal samples taken from mice from both groups, as well as from the ampicillin-sensitive AX8 microbiome from Jax.

To identify associations between bacterial taxonomy and mouse group origin, we fit multivariable linear models onto the data using MaAsLin2. Taxa significantly associated with the H47 microbiota group included many clostridial species including *Anaerostipes caccae*, *Shaedlerella arabinosiphilia*, *Enterocloster bolteae*, *Clostridium symbiosum* (**Figure 4.3A**). Other significantly enriched taxa included 2 Bacteroidota species (*Muribaculum gordoncarteri* and *Parabacteroides goldsteinii*), *Ligilactobacillus murinus*, and some *Enterococcus* species. Analysis of the H47 microbiome after treatment with ampicillin indicated that *E. bolteae* was the most significantly associated taxa (**Figure 4.3B**). Bacteria that were depleted in the H47 microbiome compared to the ampicillin-susceptible microbiomes included several species of Lactobacillaceae, as well as *Bifidobacterium pseudolongum* (**Figure 4.3A**).

To ascertain the spectrum of ampicillin sensitivity across the H47 microbiota and determine if any of the enriched species were also resistant, we cultured fecal pellets from H47 mice in media containing various concentrations of ampicillin¹⁷ (**Figure 4.3C**). We determined through 16S rRNA gene sequencing that very few bacterial species could grow out from microbiota cultures containing concentrations of ampicillin exceeding 100 mg/ml (**Figure 4.3C**), in contrast to the diverse taxonomy observed when this microbiota was exposed to ampicillin *in*

vivo (Figure 4.1D-E). Many of the bacteria that were resistant to high concentrations of

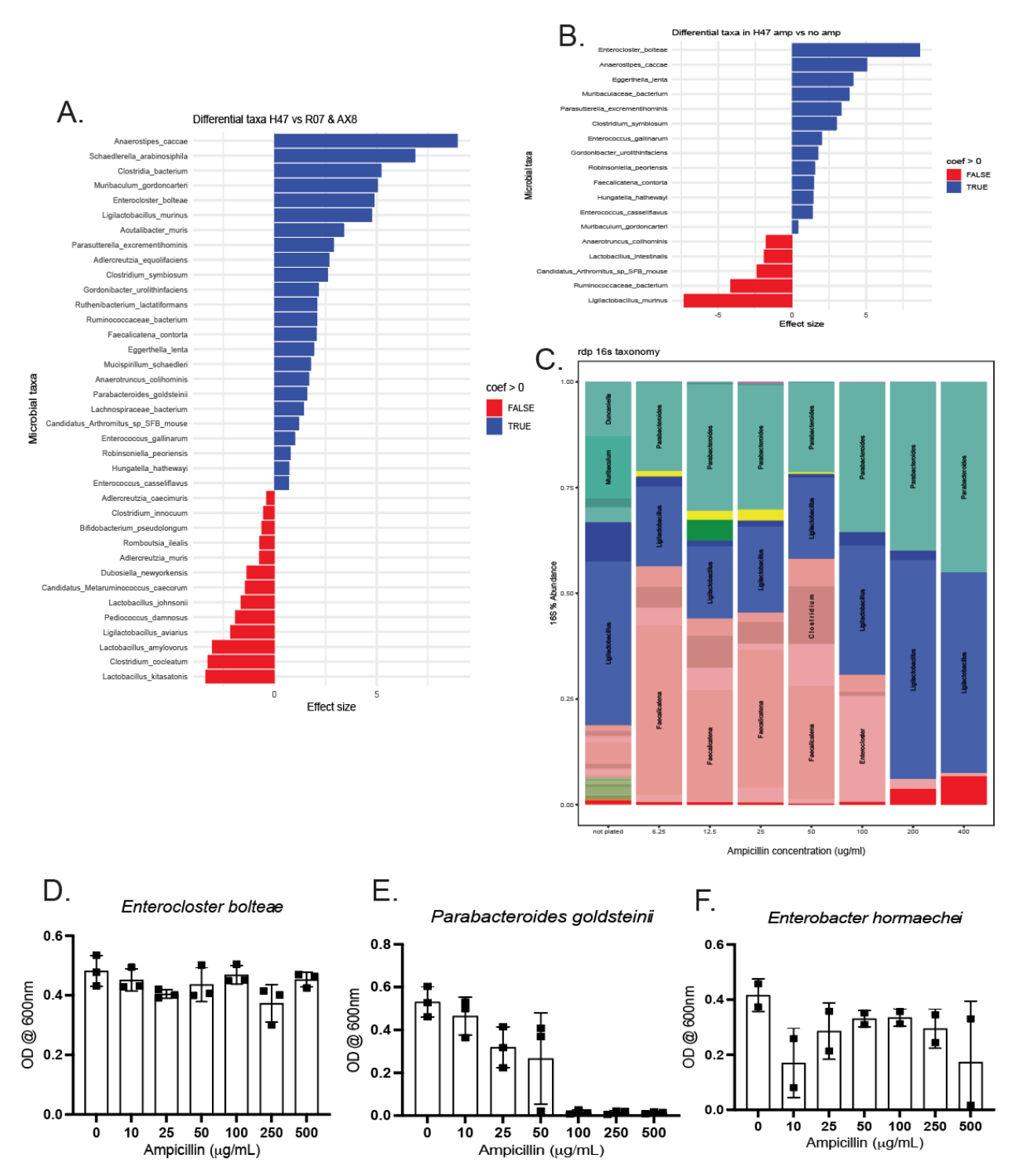


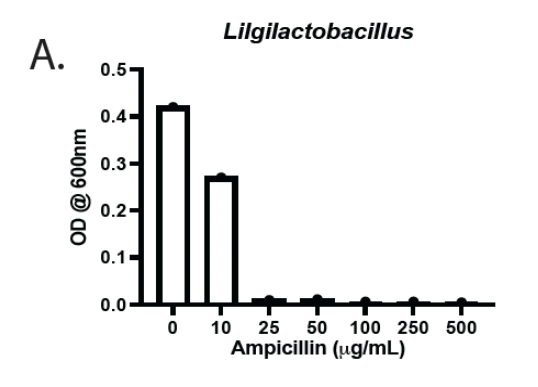
Figure 4.3. The ampicillin-resistant phenotype is found in only a few bacteria from the ampicillin-resistant microbiota of mouse group H47. A. Bacterial taxa that are significantly positively and negatively associated with the ampicillin-resistant mouse group H47, compared to the ampicillin-susceptible groups R07 and AX8, determined using MaAsLin2. Fecal

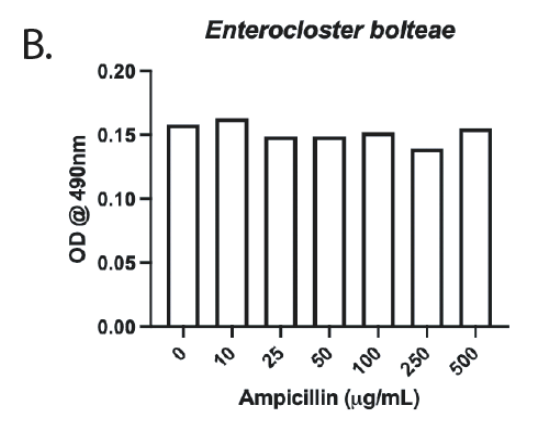
Figure 4.3 (continued) microbiomes from mouse groups include samples from before and after 3 days of ampicillin treatment. **B.** Bacterial taxa that are significantly associated with ampicillin treatment in the mouse group H47. **C.** Taxonomy of H47 fecal microbiota cultured on the indicated concentrations of ampicillin. Fecal pellets from mouse group H47 were diluted and inoculated onto BHIS plates containing ampicillin. Each bar represents 3 cultures grown in triplicate and pooled together for 16s rRNA sequencing to determine taxonomy. **D-F.** MICs of ampicillin for the indicated bacterial isolates from the fecal microbiota of mouse group H47. Bacteria were cultured overnight for 24 hours in BHIS with the indicated concentrations of ampicillin. Each symbol represents 1 individual culture, n = 3.

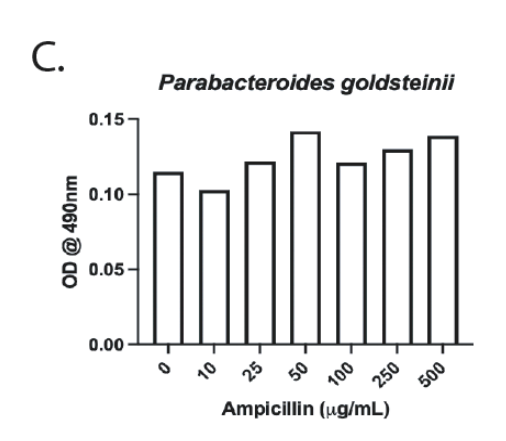
ampicillin were also identified as the most significantly associated with the H47 microbiota compared to the susceptible microbiotas tested, including *Parabacteroides goldsteinii*, *Enterocloster bolteae*, *Ligilactobacillus murinus*, and several Proteobacterial species (**Figure 4.3A-C**). Furthermore, some of these bacteria were similar species to those previously isolated from the ARM mice, like *Enterocloster bolteae* and *Parabacteroides*, despite the radically different antibiotic treatment histories of these mice¹⁷.

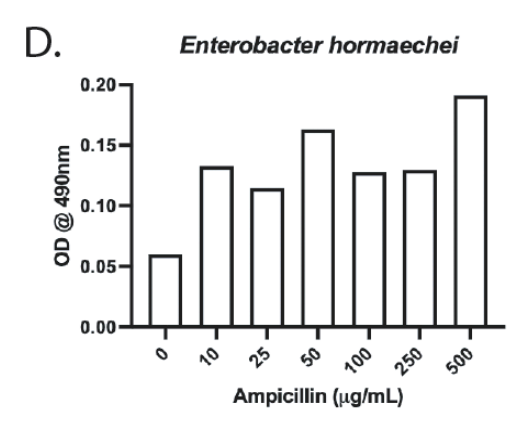
The low number of bacterial species from the H47 microbiota that were found to grow in high concentrations of ampicillin supported our hypothesis that a smaller subset of resistant bacteria were shielding the rest of the ampicillin-sensitive commensals. To test this, we isolated the bacterial strains from the H47 fecal microbiota that grew in the presence of ampicillin: *Parabacteroides goldsteinii (P. goldsteinii*_{H47}), *Enterocloster bolteae (E. bolteae*_{H47}), *Enterobacter hormaechei (E. hormaechei*_{H47}), and Ligilactobacillus murinus (L. murinus_{H47}). We determined their ampicillin MICs individually and confirmed that all isolates were ampicillin-resistant (MIC <16 mg/ml)⁶⁴, with *E. bolteae*_{H47} and *E. hormaechei*_{H47} having MICs of > 500 mg/ml, *P. goldsteinii*_{H47} having an MIC of 100 mg/ml, and *L. murinus*_{H47} having an MIC of 25 mg/ml (**Figure 4.3D-F, Figure 4.4A**). The variations in individual resistance to ampicillin

between bacterial strains is in line with previous research that has shown that bacteria are often more resistant to ampicillin when together in a community⁶⁵.









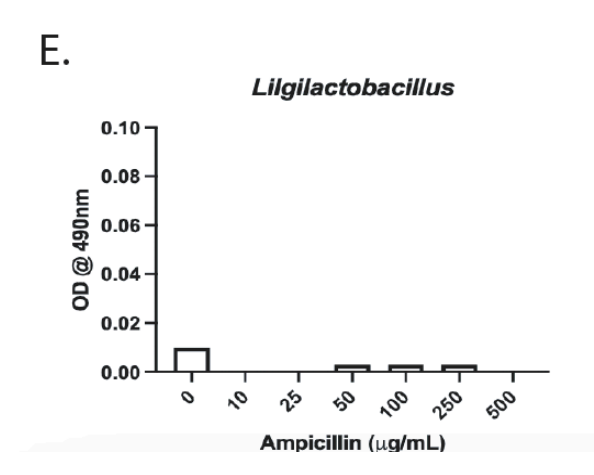


Figure 4.4 Ampicillin-resistant bacteria isolated from the fecal microbiota of mouse group H47. A. MIC of ampicillin for bacterial isolate *Ligilactobacillus murinus* from the fecal microbiota of mouse group H47. B-E. Optical density of indicated bacterial isolates cultured in ampicillin, after incubation with nitrocefin for 20 minutes.

While resistance to ampicillin in bacteria can be conferred through many genes, beta-lactamases can inactivate the ampicillin, rendering it harmless to the other commensal bacteria in the intestinal tract^{66,33}. Assessment of beta-lactamase production in each isolate by chromogenic nitrocefin assay indicated that *P. goldsteinii*_{H47}, *E. bolteae*_{H47}, and *E. hormaechei*_{H47} were all positive, while *L. murinus*_{H47} was not (**Figure 4.4B-E**). Furthermore, production of beta-lactamases was constitutive for *P. goldsteinii*_{H47} and *E. bolteae*_{H47}, but only induced in *E. hormaechei*_{H47} upon introduction of the antibiotic (**Figure 4.4B-D**).

Bacteroidales species are the most well-known members of the commensal gut microbiota to produce beta-lactamases⁶⁷, with reports describing this activity in *Bacteroides fragilis* strains dating as far back as 1955⁶⁸, though there is extreme inter-species and inter-strain variation in the presence of these genes. Beta-lactamase production is also commonly observed in *E. hormaeche*i species, which usually possess an inducible *ampC* beta-lactamase⁶⁹. However, beta-lactamase production is not as well described in *Enterocloster* bacteria, though resistance to penicillin antibiotics is common^{70,71}. We compared the ampicillin-resistance of the H47 isolates to those isolated previously from ARM, and found the *E.bolteae*_{ARM} isolate to have the same MIC (> 500 mg/ml) as the *E. bolteae*_{H47} strain (**Figure 4.4D**, **Figure 4.5A**), while *P. distasonis* ARM and *B. sartorii*_{ARM} had MICs of 250 mg/ml and 100 mg/ml, respectively (**Figure 4.5B-E**). All 3 of these isolates were also positive for beta-lactamase production by nitrocefin test (**Figure 4.5B-F**).

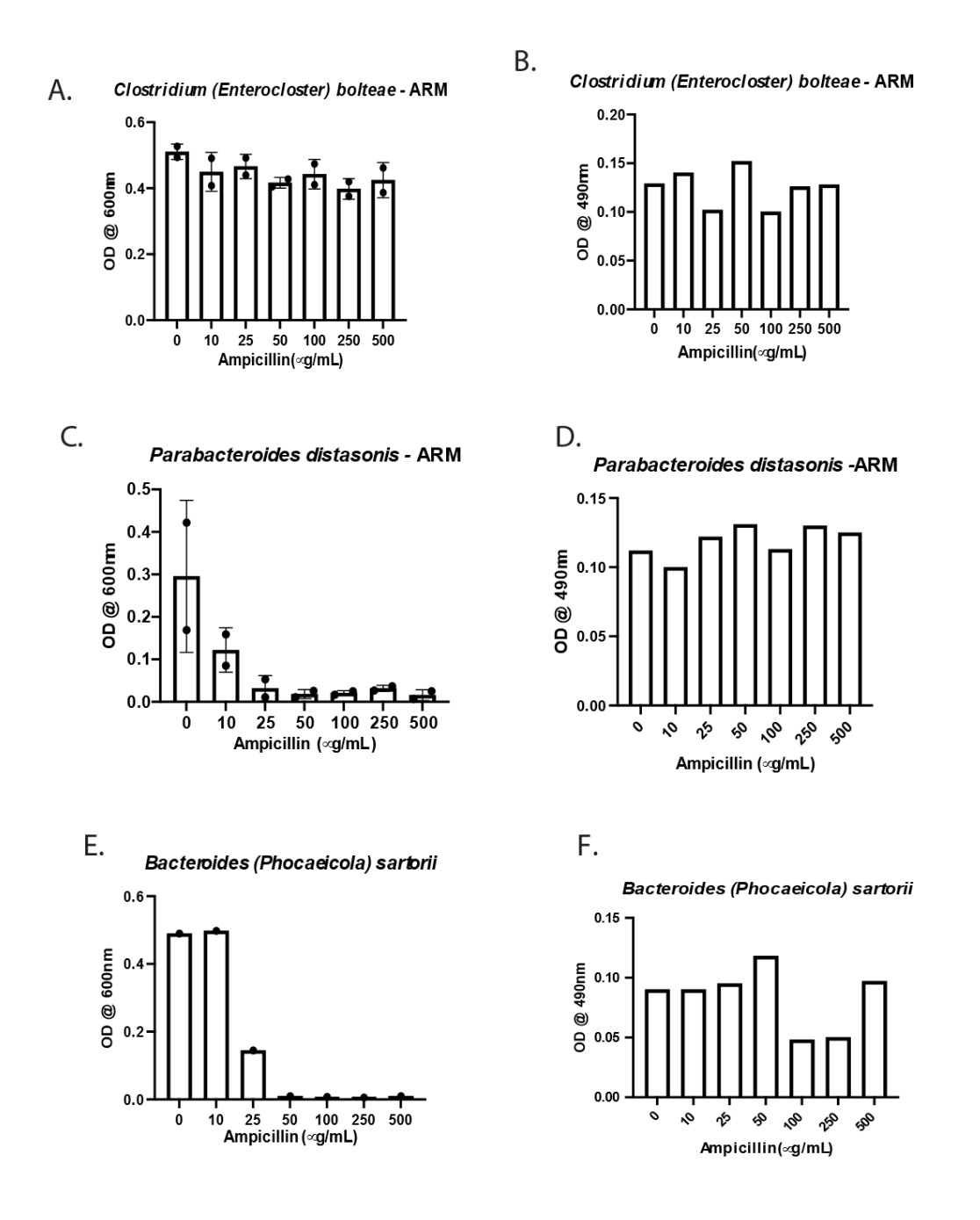


Figure 4.5 Ampicillin-resistant bacteria isolated from the fecal microbiota of the ampicillin-resistant microbiota (ARM) described in Caballero et al. A. MIC of ampicillin for bacterial isolate *Enterocloster bolteae* and B. optical density after incubation with nitrocefin for 20 minutes. C-D. *Parabacteroides distasonis* isolated from ARM, and E-F. *Bacteroides sartorii* isolated from ARM.

4.5: Beta-lactamase genes in H47 isolates

We next analyzed the genomes of the beta-lactamase positive isolates from the H47 microbiota, P. goldsteiniiH47, E. bolteaeH47, and E. hormaecheiH47, to determine which betalactamase genes were present in these bacteria. The genome of E. bolteaeH47 encoded a putative beta-lactamase gene that was identical to the blaCLO1 gene, a beta-lactamase identified in several strains of E. bolteae and E. clostridioformis⁷². This same gene was also previously found in an integrative conjugative element (ICE) identified in E. clostridioformis, however the rest of the ICE was not found in the previously studied E. bolteae isolates⁷². The E. bolteae $_{H47}$ strain shared only part of the integrase core domain, upstream of the blaCLO1 gene, with the E. clostridioformis ICE. However, these were flanked by relaxase and resolvase enzymes, suggesting potential for horizontal transfer of this gene^{73,74}. The closest related clostridial betalactamase gene to the E. bolteaeH47 blaCLO1 gene here was the blaCBP-1 gene (65% identity), a class A beta-lactamase identified from a beta-lactam resistant *Clostridium botulinum* isolate. The C. botulinum genome had 2 regulatory genes downstream, in the same orientation as blaCBP-1⁷⁵. Similarly, we located 2 beta-lactamase regulatory genes downstream of blaCLO1 in the same orientation, suggesting that this is a common feature for beta-lactamase genes of this phylum (Figure 4.6).

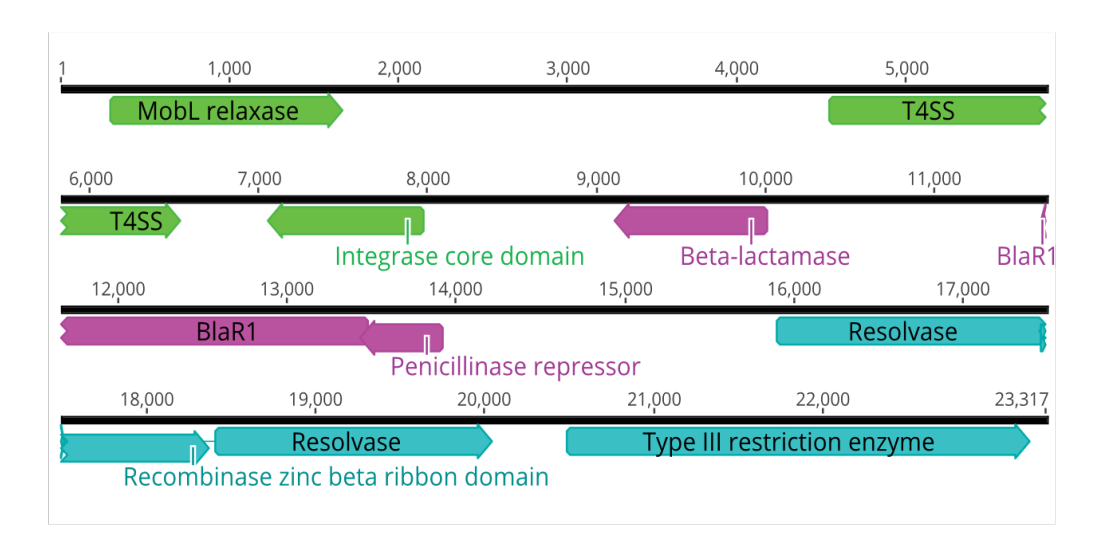


Figure 4.6 Structure of the putative *bla*CLO1 gene operon from *Enterocloster bolteae*_{H47}. The sequence for the blaCLO1 beta-lactamase gene and nearby elements suggestive of horizontal gene transfer, annotated using NCBI BLAST and Pfam domain homology.

We analyzed metagenomic short reads from the fecal microbiomes of mice from H47 before and after they were treated with ampicillin and discovered that the *bla*CLO1 gene operon was only detected after ampicillin treatment (**Figure 4.7A**). This beta-lactamase operon was not found in the microbiomes of R07 or AX8 mice, in line with their susceptibility to ampicillin (**Figure 4.7A, 4.1G**). *Enterocloster bolteae* is known to be a part of the healthy human gut microbiota⁷², prompting us to look for this gene operon in bacteria isolated from healthy human donors⁷⁶. We found an identical *bla*CLO1 operon in a *Lacrimispora* isolate, a closely related Lachnospiraceae species, as well as similar *bla*CLO1 operons in *E. bolteae* and *E. clostridioformis* (**Figure 4B**). This suggests that the *bla*CLO1 gene is present in the healthy human commensal gut microbiome. We also found the same *bla*CLO1 operon in the *E.bolteae*_{ARM} genome, consistent with their equivalent ampicillin MICs (**Figure 4.7B, 4.5A**).

Genomic analysis of the P. goldsteiniiH47 bacterial isolate revealed that this genome harbored a putative blaMUN gene, a family of class A beta-lactamases found in several different Bacteroidales species⁷⁷. The blaMUN gene from the *P. goldsteiniiH47* was similar in length and most similar in homology to the blaMUN gene identified previously in a human P. goldsteinii isolate⁷⁸. However, homology was low enough that the blaMUN is likely a distinct gene variant within this family of beta-lactamases (Figure 4.7D). As was the case with blaCLO1, blaMUN was only detected in microbiome samples from H47 mice that were first exposed to ampicillin (Figure 4.7C). Comparison of the P. goldsteiniiH47 blaMUN gene to the Bacteroidales genomes of healthy human donor isolates⁷⁹ demonstrated that similar MUN family genes were present, but distinct from those derived from *Parabacteroides goldsteinii* species (Figure 4.7D). Similar analysis of the E. hormaechei genome found that this isolate possessed a variant of the ACT gene, an inducible ampC beta-lactamase⁸⁰, that was found in H47 ampicillin-treated microbiome samples (Figure 4.7E). Similar ampC ACT genes were also detected in Enterobacteriaceae bacteria isolated from healthy humans, such as E. coli and Citrobacter (Figure 4.7F). These results suggest that the beta-lactamase genes found in the H47 microbiome are uncommon for mouse microbiomes, but not exclusively unique to mouse-derived commensal bacteria.

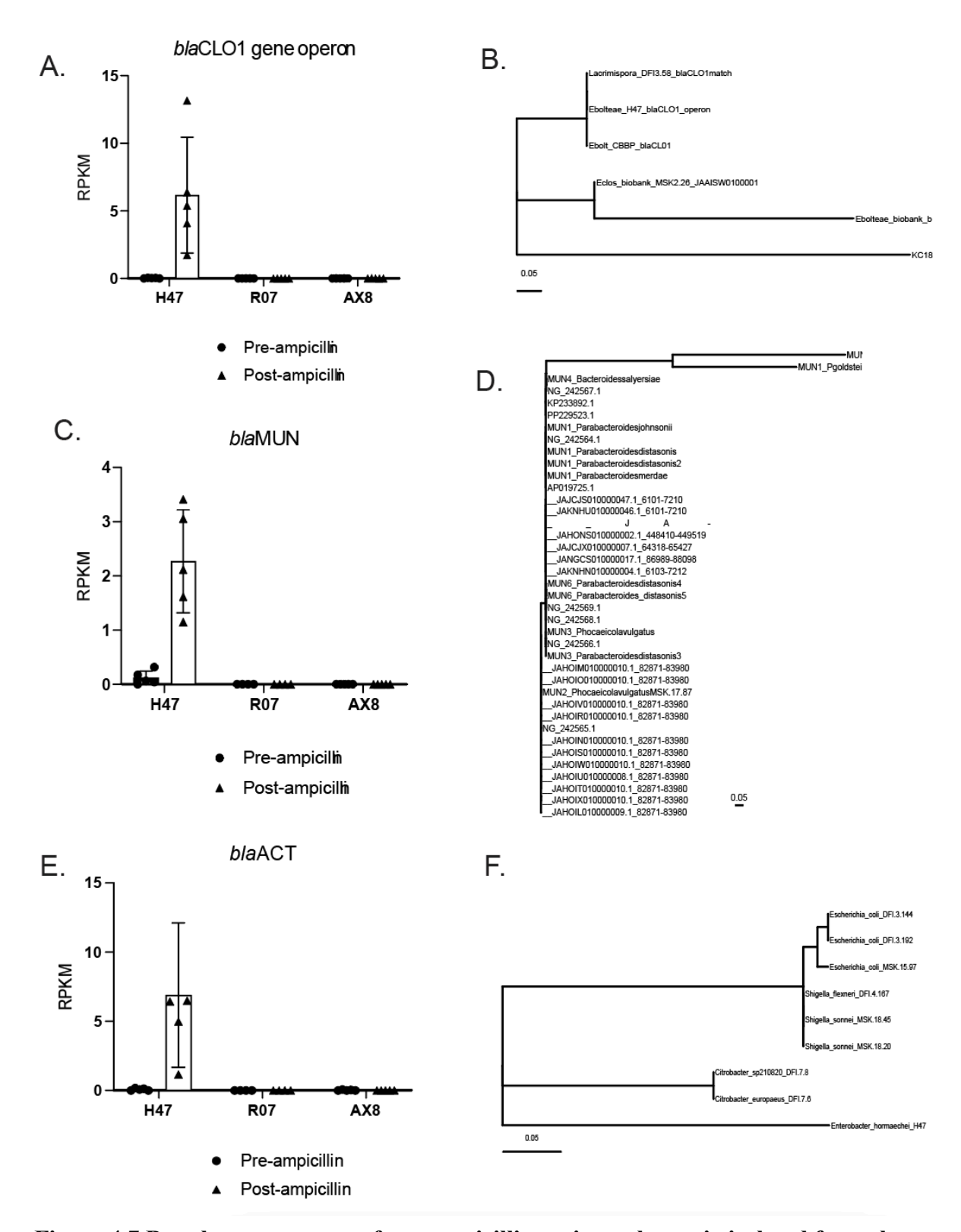


Figure 4.7 Beta-lactamase genes from ampicillin-resistant bacteria isolated from the fecal microbiota of mouse group H47. A. Reads per kilobase per million mapped reads from the fecal metagenomes of the indicated mouse groups to the gene operon *bla*CLO1

Figure 4.7 (continued) from the *Enterocloster bolteae* isolate. **B.** Phylogenetic tree of the evolutionary relationship between the *bla*CLO1gene in **A.** from the *E. bolteae*_{H47} isolated and the related genes from bacteria isolated from healthy human donor feces. **C.** Reads per kilobase per million mapped reads from the fecal metagenomes of the indicated mouse groups to the *bla*MUN gene from the *Parabacteroides goldsteinii* isolate, and **D.** phylogenetic tree of the evolutionary relationship between that gene and related genes from other Bacteroidales species isolated from healthy human donors. **E.** Reads per kilobase per million mapped reads from the fecal metagenomes of the indicated mouse groups to the gene *bla*ACT from the *Enterobacter hormaechei* isolate, and **F.** phylogenetic tree comparing this gene to related genes from commensals of healthy humans.

4.6 Ampicillin-resistant microbiomes retain their colonization resistance to opportunistic pathogens

The major negative consequence of antibiotic-treatment in patients is the loss of colonization resistance to opportunistic pathogens that can go on to dominate the intestine². To investigate if resistance to ampicillin-mediated dysbiosis also rendered H47 mice resistant to infection with vancomycin-resistant *Enterococcus faecium* (VRE), we challenged mice while they were undergoing ampicillin treatment (**Figure 4.8A**). Assessment of intestinal burden post-infection showed that H47 mice were totally resistant, while challenge of mice from ampicillin-sensitive groups showed consistently high pathogen burdens (**Figure 4.8B**). These results were further corroborated by analysis of the fecal microbiota composition after infection by 16s rRNA-sequencing, which indicated that mice with microbiota susceptible to ampicillin-mediated dysbiosis became dominated by VRE, while H47 mice remained pathogen-free (**Figure 4.8D**). To determine if the colonization resistance H47 mice exhibited towards VRE was specific to the pathogen, we challenged mice with *Klebsiella pneumoniae* (CRKp). Just as we saw with VRE,

the mice from group H47 were resistant to infection with CRKp, while all of the mice with ampicillin-sensitive microbiomes became heavily dominated (**Figure 4.8C-E**).

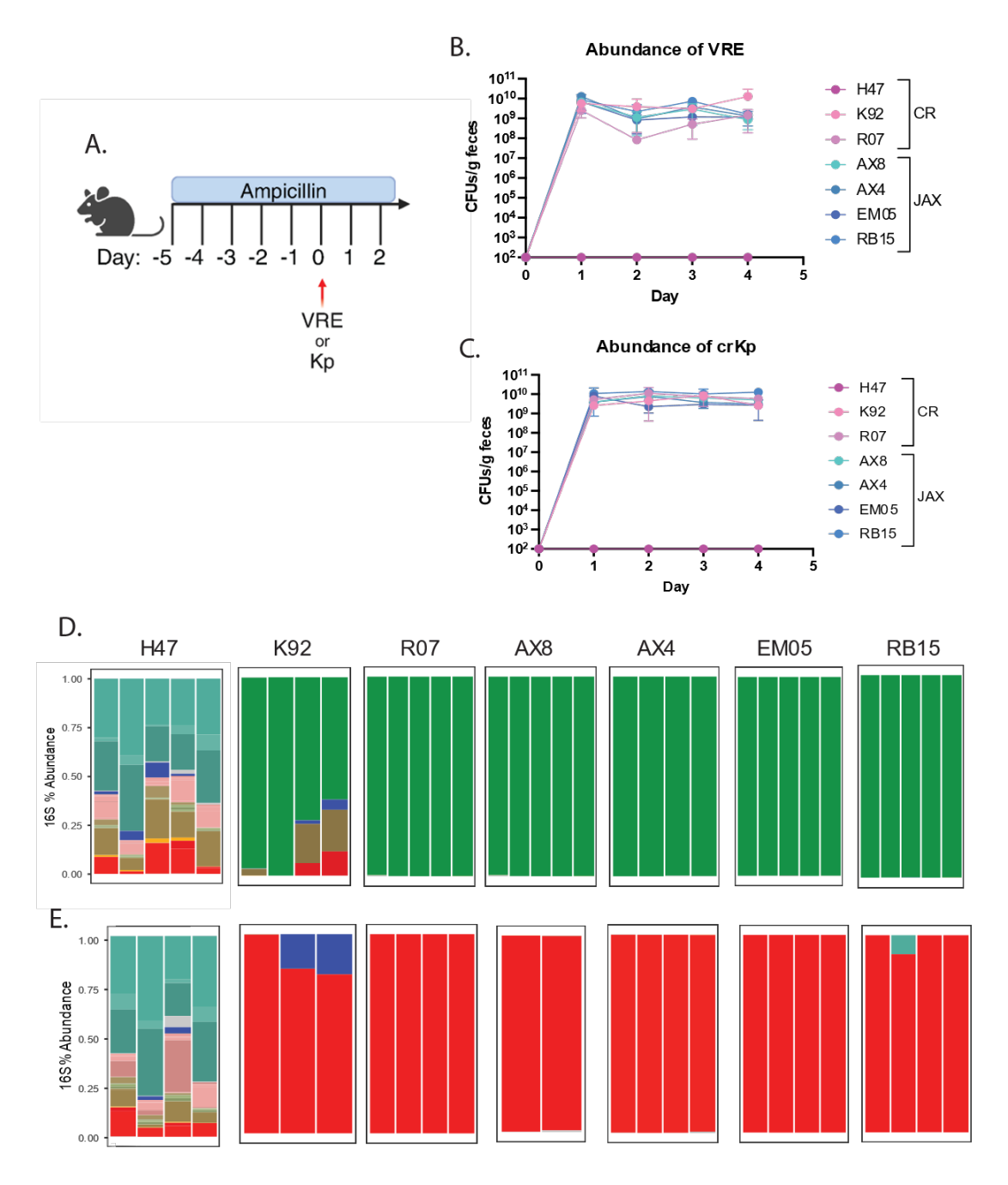


Figure 4.8 Resistance to ampicillin-mediated dysbiosis enables resistance to infection. A. Experimental timeline. Mice were treated with 0.5g/L of ampicillin in their drinking water for the duration of the experiment. After 5 days of ampicillin treatment, mice were

Figure 4.8 (continued) orally infected with 10⁶ CFUs of either vancomycin-resistant *Enterococcus* (VRE) or carbapenem-resistant *Klebsiella pneumonia* (crKp). **B.** Abundance of VRE or **C.** crKp in fecal pellets of mice from each mouse group, as determined by culturing of fecal pellets on differential and selective agar. **B-C.** Each symbol is the average of 3-5 mice. **D.** Taxonomic composition of the fecal microbiomes of mice from each group on day 4 post-infection with VRE or **E.** crKp. Each bar represents the individual fecal microbiome of a single-housed mouse.

These results suggest that resistance to ampicillin-induced disruption enabled H47 mice to maintain colonization resistance to these different pathobionts, a hallmark of a healthy gut microbiota^{50,2}. While the ampicillin-resistant isolates from the H47 microbiome were similar to those isolated from the previously characterized ARM mice⁸¹, they failed to directly kill VRE *in vitro* like the ARM consortium (**Figure 4.9**), which contained an ampicillin-sensitive lantibiotic-producing *Blautia producta* species^{16,16}. This was consistent with colonization resistance in H47 being mediated by their resistance to ampicillin-induced dysbiosis.

We hypothesized that the beta-lactamase producing bacteria isolated from the H47 microbiota were sufficient to confer protection to the rest of the ampicillin-sensitive bacteria in the gut. To test this, we administered fecal microbiota transplants (FMTs) to germ-free mice to associate them with the ampicillin-sensitive fecal microbiota of AX8 mice, with or without the 3-member ampicillin-resistant consortium from H47. The AX8 microbiota was significantly different in composition to the H47 mice, partially likely due to the drift in their genetic backgrounds⁸².

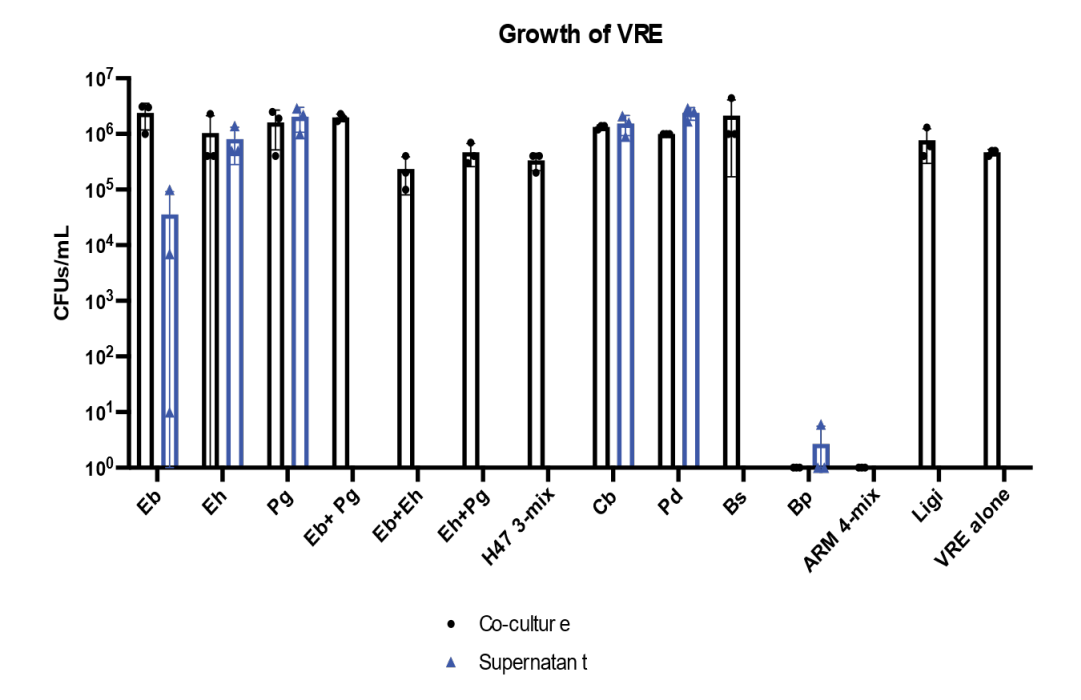


Figure 4.9 Suppression of VRE growth *in vitro* by bacterial isolates from the fecal microbiota of mouse group's H47 and ARM. Bacterial isolates were grown under anaerobic conditions, individually in supplemented BHI. For co-culture tests (black circles), stationary phase cultures of bacterial isolates were normalized to the same OD, and then ~100 CFUs of VRE was added to 1 mL of each culture. For supernatants (blue triangles), 1 mL of supernatant from stationary phase cultures of bacterial isolates was inoculated with ~100 CFUs of VRE. After being incubated anaerobically overnight at 37°C, cultures were diluted 10-fold, plated onto Difco Enterococcosel agar, and then incubated overnight at 37°C for enumeration of VRE CFUs. Each symbol represents an individual culture.

Recipient mice were then treated with ampicillin, followed by VRE challenge (**Figure 4.10A**). Mice associated with only the AX8 microbiota were susceptible to ampicillin-induced dysbiosis, as demonstrated by their enlarged ceca (**Figure 4.10B-D**). This dysbiosis subsequently rendered mice susceptible to dense colonization with VRE (**Figure 4.10E**), consistent with the susceptibility shown by the mice the microbiota originated from (**Figure 4.8A**). In contrast, when the AX8-derived FMT was augmented with the 3-member H47 consortium, recipient mice

were resistant to ampicillin-mediated gut dysbiosis, as evidenced by their lower cecal weight and resistance to VRE (**Figure 4.10C-E**). These results suggest that a small subset of beta-lactamase

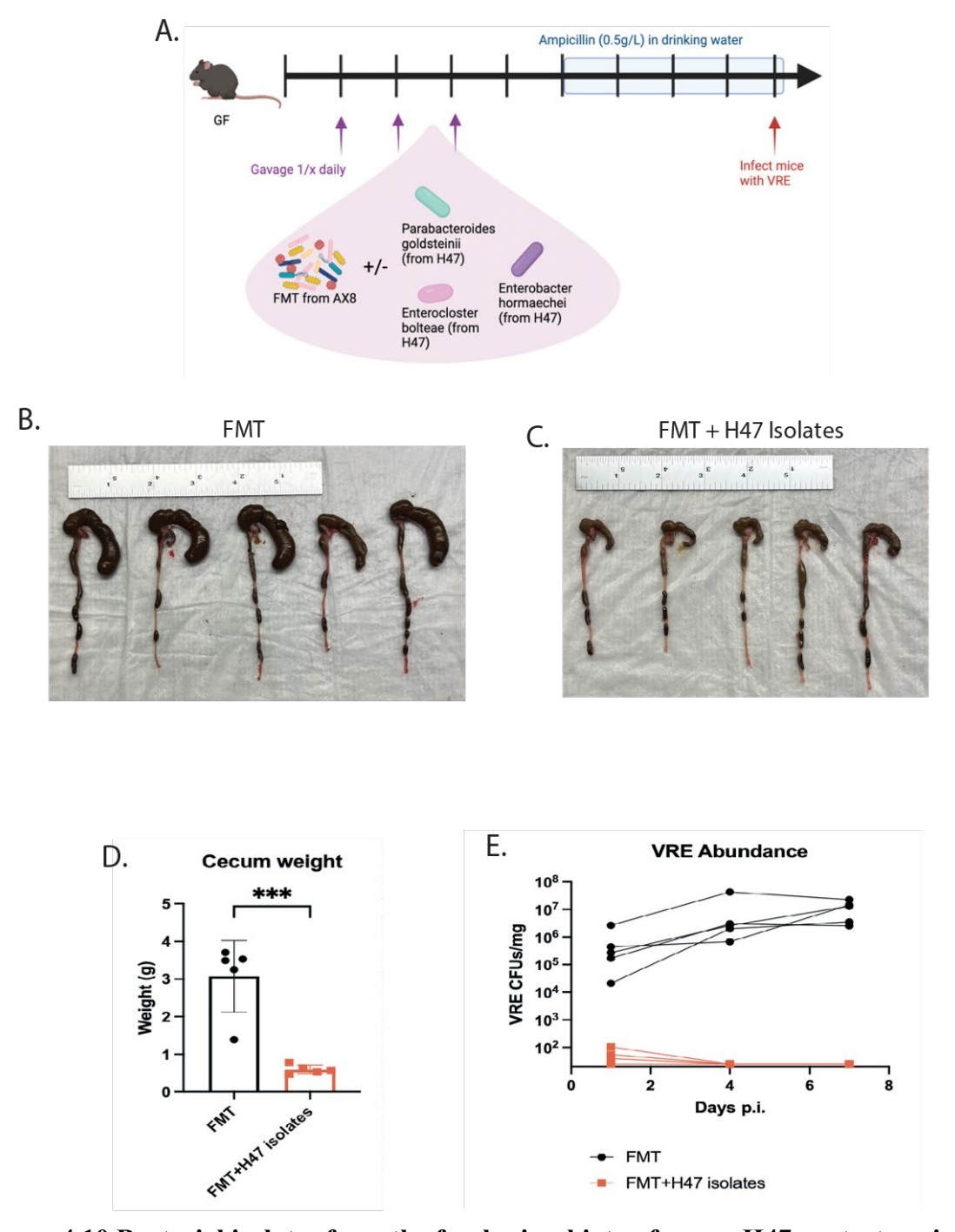


Figure 4.10 Bacterial isolates from the fecal microbiota of group H47 protect against ampicillin-induced dysbiosis and subsequent VRE infection. A. Experimental design. Individually-housed germ-free (GF) mice were given a fecal microbiota transplant (FMT)

Figure 4.10 (continued) from the ampicillin-susceptible microbiome of group AX8 with or without the 3 additional bacterial species *Entercloster bolteae*, *Parabacteroides goldsteinii*, *Enterobacter hormaechei* isolated from the fecal microbiota of group H47. Mice were then treated with ampicillin (0.5g/L) in their drinking water for 4 days before oral challenge with VRE, and maintained this antibiotic regimen for the duration of the experiment. **B.** Photo of the ceca of mice associated with FMT from AX8 alone or **C.** FMT from AX8 supplemented with the 3 isolates from H47, 7 days post-infection with VRE. **D.** Cecal weights of each mouse shown in **B-C. E.** Abundance of VRE in the fecal pellets of mice over time, as determined by culturing on selective and differential agar. **D-E.** Each symbol represents a single mouse, mice treated with FMT from AX8 alone are in black and mice treated with FMT from AX8 supplemented with the 3 isolates are in red.

producing bacterial strains can protect ampicillin-sensitive members of the microbiota from ampicillin-induced dysbiosis and maintain colonization resistance to opportunistic pathogens.

These studies further our understanding of antibiotic-resistance in the commensal gut microbiota, specifically in the context of sensitivity to ampicillin.

4.7 Summary of results

This study demonstrates that resistance to ampicillin can be found in microbiota without a long history of ampicillin treatment, and that a small number of species from this microbiota are sufficient to transfer this resistance to an ampicillin-sensitive microbiota. We identified the protective members of the H47 microbiota, isolated them, and characterized them genetically and functionally. The ability for this H47-derived consortium to protect an ampicillin-sensitive microbiota that differed significantly in composition suggests that there is potential in using this

consortium for probiotic purposes. We also identified bacterial isolates from human donors with similar beta-lactamase genes, indicating that the ampicillin-resistance phenotype is not unique to mice and can be detected in humans. These findings highlight the importance of antibiotic-resistance in commensal bacteria and potential to protect from the microbiota from dysbiosis and subsequent opportunistic infections.

CHAPTER 5: Discussion

5.1.1 Conclusions on prevention of coprophagy in mice during homeostasis and VRE infection

In these experiments, we utilized a novel tail cup device that prevents coprophagia in mice to investigate how colonization resistance to VRE is mediated in the small vs. large intestine. We found that after antibiotic treatment, VRE is able to densely colonize the SI, forming small clusters along the epithelium. Furthermore, we saw that de-colonization of the SI precedes clearance of VRE from the colon, suggesting that resistance in this niche is formed separately.

Before introducing VRE into mice, we characterized the effects of the tail cups on the mice to ensure that we were able to replicate the phenotypes observed by the original tail cup designers. Though we observed the same effects on the composition and density of the microbiota throughout the GI tract, we also had some differences in key findings. Importantly, mice in our experiments did not experience weight loss, which was a concerning finding from the original designers in mice wearing both functional and non-functional mock cup devices. This could be due to multiple reasons: such as differences in the actual fit of the tail cup, the layout of the cage interfering with food access while in the cups, or differences in the nutrition values between diets.

We also observed some differences in our measurements of bile acids throughout the gut, although direct comparison between experiments is made difficult by the method of pooling used in their measurement and analysis. Bogatyrev et al. observed an increase in the overall pool of conjugated bile acids of non-coprophagic mice, and a matching decrease in the deconjugated

pool of bile acids. In our experiments however, we measured a decrease in the glycine-conjugated primary bile acids (PBAs) in the SI of tail cup mice, along with the decrease in deconjugated PBAs observed by the previous group. Glycine-conjugates are more common in humans than mice²⁴, and the concentration of these conjugates is many log-folds below the PBAs conjugated to taurine, which are so high they are outside of the range of reliable quantification. Since there are much lower concentrations in the glycine-conjugated PBAs, the more modest shifts in their concentration is easier to measure.

The change in glycine-conjugated PBAs was surprising to see though, as these are synthesized by the liver, being secreted directly into the duodenum after ingestion of meals to help with digestion⁴³. The decrease in PBAs suggests potential changes in tail cup mice to the reabsorption rates of bile acids through their SI and back into hepato-circulation, or changes in their overall synthesis rates. Since secretion of conjugated PBAs into the duodenum is a result of eating, it is also possible that mice in mock cups have increased secretion of PBAs into their SI as a result of ingestion of feces. Further studies into how coprophagia influences gallbladder storage will be critical for clarifying the reasons for these differences in PBA conjugates.

We also saw significant differences in the amount of secondary bile acids (SBAs) measured in the SI of mice from both groups. The original group saw no significant changes in the amount of SBAs between mouse groups; and similar measurements throughout the GI tract. In contrast, we saw that there were very few samples with quantifiable SBAs in their SI, although the few that did were all coprophagic. For the most part though, we did not observe dramatic differences in the SBAs of the LI. This could again potentially be a result of pooling together the various SBA compounds, obscuring the subtle differences in different compounds.

Previous studies from our lab have demonstrated that Reg3g from the SI is critical for restriction of VRE in the GI tract, so we focused our investigations here on this bactericidal lectin. This change in microbiome composition of the SI of tail cup mice suggests that the bacteria that actually engraft in the SI are much less diverse than what is typically seen in standard coprophagic mouse studies. The consequence of this shift in bacteria can be immediately measured by the decrease in Reg3g expression of SPF mice in tail cups.

However, the ability for mice in tail cups to eliminate VRE from their ileums more quickly than their mock counterparts suggests that their lower Reg3g levels were still sufficient to help re-establish colonization resistance. This is potentially due to the shift in VRE colonization kinetics from the lack of coprophagia. Since the Reg3g is working on a finite pool of VRE in the tail cup mice, it likely takes less Reg3g to accomplish the task of removing the VRE that engrafted into the SI upon infection. Conversely, coprophagia increases the small intestinal pool of VRE, leading to VRE recycled from the LI to constantly pass through the SI, creating more potential opportunities for engraftment, and overall taking longer for decolonization of the whole GI tract.

5.1.2 Limitations and Outlook

There are several potential barriers to the adoption of these functional tail cup devices as a universal standard in microbiome mouse models. As the tail cups are currently designed, they are not ideal for use with female mice due to the placement of their urethra, and modifications would be required to allow for unimpeded urination of female mice. Another obstacle is the

time-cost to the researcher, as use of functional tail cups requires daily emptying and cleaning of the feces that accumulates in the cup. Daily handling during experiments is also not ideal due to the stress it can cause on the animals, so a design that allows for longer periods between cup emptying would be better for longer-term experiments. The overall duration of the experiments is another potential issue with using these cups, as our studies here (and former studies with the cup) did not keep mice in cups for longer than a few weeks. While some mice appeared undisturbed by the prolonged cup use, some mice overgroomed at the site of contact with the cup rim, which could be an indication of discomfort in some animals, especially over time.

Despite the potential issues, utilization of the tail cup devices illustrated how coprophagia is a radical perturbation of the SI that is not typically seen in healthy humans. The tail cup devices dramatically altered the microbial and immune landscape of mice, creating a biogeographic distribution of bacteria much more in line with what is seen in humans⁴². In most experimental mouse microbiome models, coprophagia is usually accounted for by individually-housing mice to prevent contamination of microbiota between cage mates. However, self-reinoculation of pathogens is much harder to control for, and contributes to the heterogeneity seen when quantifying VRE levels of coprophagic mice. Use of tail cup devices presents a useful opportunity for the researcher to control this variable, further standardizing outcomes across samples.

The use of these tail cups gave us the unique opportunity to characterize the colonization of *E. faecium* in the mouse ileum undisturbed by coprophagia, enabling us to visualize the heterogeneity in engraftment of the bacteria along the GI tract. The close associations of these bacteria with the epithelium that we saw illustrate how Reg3g would have the ability to come into contact with *E. faecium* and remove the bacteria from this niche, because it is secreted

directly by the SI epithelium. Our finding that VRE could not engraft into any part of the GI tract of non-antibiotic treated SPF mice contradicts previous findings into naïve and antibiotic-treated mice challenged with VRE ⁴. However, this is more reflective of what we see in human patient populations, wherein patients only become susceptible after treatment with antibiotics, and healthy people with a diverse microbiota are not susceptible to colonization¹.

5.2.1 Conclusions on ampicillin-resistant bacterial consortia

Our goal for these experiments was to probe the ampicillin-sensitivity of a random assortment of healthy microbiota, identifying and isolating resistant bacteria that can be built into protective consortia. We were lucky to identify a single resistant mouse colony group, H47 from Charles River, out of the 7 different colonies tested. Surprisingly, the composition of the ampicillin-resistant bacterial consortium isolated from the H47 microbiota was similar to the resistant consortium we isolated previously, with the inclusion of an *E. bolteae* species and a Bacteroidales bacterium. In the case of this previous consortium, we only tested ampicillin-resistance and beta-lactamase production in *B. sartorii*ARM and *P. distasonis*ARM¹⁷, as this bacterial phylum is much more commonly associated with beta-lactamase expression⁸³. Furthermore, when assessing the roles of each bacterium in that consortium, it was not clear how *E. bolteae*ARM was assisting the ampicillin-sensitive *B. producta*ARM in engrafting in the ampicillin-treated mouse gut. We speculate now that this member also participated in depletion of ampicillin in the gut, allowing persistence of the more sensitive *B. producta*ARM consortium member during ampicillin treatment. The similarity in composition of these

ampicillin-degrading bacterial consortia isolated from resistant mouse colonies suggests that the phenotype of ampicillin-resistance can be achieved with combinations of these bacterial species. We can use this as a guiding principle in the rational design of beta-lactamase producing bacterial consortium to be used therapeutically.

Though the microbiota of H47 mice was resistant to overall depletion in their abundance and diversity of bacteria, the changes we observed in their metabolite production is suggestive of the shift in function the microbiome undergoes during ampicillin treatment. The significant reduction in 5-aminovalerate (5-AV) could be caused directly by changes in the fermentation habits of the ampicillin-resistant bacteria, or indirectly from the change in metabolites available for cross-feeding of other bacteria⁴⁴. The slight reductions in secondary bile acids such as 3-oxo-LCA and iso-allo-LCA could potentially also have effects on the intestinal immune system²⁶, so the full effects of this consortium on the host should be explored.

Interestingly, these studies show though that active treatment with ampicillin is not required for these bacterial isolates to persist in their complex microbiota, however some of them become enriched after treatment. The evolutionary advantage of harboring such genes without the active selection pressure of antibiotics is unclear, but research has demonstrated that these genes can persist in healthy humans long after the cessation of antibiotics⁸⁴.

The 3 ampicillin-resistant bacteria isolated from H47 are all species not typically associated with mice, and instead are usually found in human microbiota. It is therefore likely that the H47 mice acquired these bacterial species from their human handlers. Further supporting this idea, similar beta-lactamase genes were detected in the genomes of bacteria isolated from healthy human donors. Studies have shown that humans in industrialized nations are reservoirs for harboring antibiotic-resistant bacteria ^{85,86}.

5.2.2 Limitations and Outlook

The beta-lactamase genes identified in the 3 bacterial isolates from H47 became enriched in their fecal metagenomes during exposure to ampicillin, suggesting that the antibiotic treatment selects for these genes. This could imply that the genes are being spread to other bacteria within the gut; supporting this, some mobile genetic elements were found in the blaCLO1 gene operon. The presence of the antibiotic also activates regulators and other inducible sensors within the bacteria themselves that leads to an increase in their individual production of beta-lactamases⁸⁷. A limitation of these studies is that without long-read sequencing, it is hard to confidently assign these genes to specific metagenome-assembled genomes.

Whether or not all of the isolates derived from the H47 microbiota can be considered true "commensals" is complicated, as *Enterobacter hormaechei* is a part of the *Enterobacter cloacae* complex (ECC), a group of bacteria generally thought of more as opportunistic pathogens, due to their associations with hospital-associated infection⁸⁸. However, the antibiotic-resistance genes commonly associated with virulence in these bacteria are absent in our H47 isolate strain, including class D beta-lactamases that hydrolyze carbapenems or extended spectrum beta-lactamases^{69,89}. Furthermore, *E. hormaechei* can be found in natural environments, including on plants and insects^{90,91}, which is indicative of their potential as more benign members of microbial communities.

Moving forward, it will be interesting to see if these isolates from H47 can be combined to protect human gut microbiota that are sensitive to ampicillin. These studies also provide a blueprint for investigating the phenomena of beta-lactamase mediated resistance in non-antibiotic treated healthy human samples.

<u>REFERENCES</u>

- 1. Arias, C. A. & Murray, B. E. The rise of the Enterococcus: beyond vancomycin resistance.

 Nat. Rev. Microbiol. 10, 266–278 (2012).
- 2. Buffie, C. G. & Pamer, E. G. Microbiota-mediated colonization resistance against intestinal pathogens. *Nat. Rev. Immunol.* **13**, 790–801 (2013).
- 3. Khan, N. *et al.* Fecal microbiota diversity disruption and clinical outcomes after auto-HCT: a multicenter observational study. *Blood* **137**, 1527–1537 (2021).
- Ubeda, C. et al. Vancomycin-resistant Enterococcus domination of intestinal microbiota is enabled by antibiotic treatment in mice and precedes bloodstream invasion in humans. J. Clin. Invest. 120, 4332–4341 (2010).
- 5. Peled, J. U. *et al.* Microbiota as Predictor of Mortality in Allogeneic Hematopoietic-Cell Transplantation. *N. Engl. J. Med.* **382**, 822–834 (2020).
- Gao, W., Howden, B. P. & Stinear, T. P. Evolution of virulence in Enterococcus faecium, a hospital-adapted opportunistic pathogen. *Host-Pathog. Interact. Evol. Regul. Host Pathog. Interact.* 41, 76–82 (2018).
- 7. Lebreton, F. *et al.* Tracing the Enterococci from Paleozoic Origins to the Hospital. *Cell* **169**, 849-861.e13 (2017).
- Staley, C., Dunny, G. M. & Sadowsky, M. J. Chapter Four Environmental and Animal-Associated Enterococci. in *Advances in Applied Microbiology* (eds. Sariaslani, S. & Gadd, G. M.) vol. 87 147–186 (Academic Press, 2014).
- 9. Sorbara, M. T. & Pamer, E. G. Interbacterial mechanisms of colonization resistance and the strategies pathogens use to overcome them. *Mucosal Immunol.* **12**, 1–9 (2019).

- 10. Krawczyk, B., Wityk, P., Gałęcka, M. & Michalik, M. The Many Faces of Enterococcus spp.—Commensal, Probiotic and Opportunistic Pathogen. *Microorganisms* **9**, (2021).
- 11. Reyes, K., Bardossy, A. C. & Zervos, M. Vancomycin-Resistant Enterococci. *Infect. Dis. Clin. North Am.* **30**, 953–965 (2016).
- 12. Dubin, K. A. *et al.* Diversification and Evolution of Vancomycin-Resistant Enterococcus faecium during Intestinal Domination. *Infect. Immun.* **87**, e00102-19 (2019).
- 13. Kayama, H., Okumura, R. & Takeda, K. Interaction Between the Microbiota, Epithelia, and Immune Cells in the Intestine. *Annu. Rev. Immunol.* **38**, 23–48 (2020).
- 14. Buffie, C. G. *et al.* Precision microbiome reconstitution restores bile acid mediated resistance to Clostridium difficile. *Nature* **517**, 205–208 (2015).
- 15. Brandl, K., Plitas, G., Schnabl, B., DeMatteo, R. P. & Pamer, E. G. MyD88-mediated signals induce the bactericidal lectin RegIIIγ and protect mice against intestinal *Listeria monocytogenes* infection. *J. Exp. Med.* **204**, 1891–1900 (2007).
- 16. Kim, S. G. *et al.* Microbiota-derived lantibiotic restores resistance against vancomycin-resistant Enterococcus. *Nature* **572**, 665–669 (2019).
- 17. Caballero, S. *et al.* Cooperating Commensals Restore Colonization Resistance to Vancomycin-Resistant Enterococcus faecium. *Cell Host Microbe* **21**, 592-602.e4 (2017).
- 18. Thaiss, C. A., Zmora, N., Levy, M. & Elinav, E. The microbiome and innate immunity.

 Nature 535, 65–74 (2016).
- 19. Kinnebrew, M. A. *et al.* Bacterial flagellin stimulates toll-like receptor 5—dependent defense against vancomycin-resistant Enterococcus infection. *J. Infect. Dis.* **201**, 534–543 (2010).
- 20. Abt Michael C. *et al.* TLR-7 activation enhances IL-22–mediated colonization resistance against vancomycin-resistant enterococcus. *Sci. Transl. Med.* **8**, 327ra25-327ra25 (2016).

- 21. Brandl, K. *et al.* Vancomycin-resistant enterococci exploit antibiotic-induced innate immune deficits. *Nature* **455**, 804–807 (2008).
- 22. Kinnebrew, M. A. *et al.* Interleukin 23 Production by Intestinal CD103+CD11b+ Dendritic Cells in Response to Bacterial Flagellin Enhances Mucosal Innate Immune Defense. *Immunity* 36, 276–287 (2012).
- 23. Collins, S. L., Stine, J. G., Bisanz, J. E., Okafor, C. D. & Patterson, A. D. Bile acids and the gut microbiota: metabolic interactions and impacts on disease. *Nat. Rev. Microbiol.* **21**, 236–247 (2023).
- 24. Mohanty, I. *et al.* The changing metabolic landscape of bile acids keys to metabolism and immune regulation. *Nat. Rev. Gastroenterol. Hepatol.* **21**, 493–516 (2024).
- 25. Paik, D. *et al.* Human gut bacteria produce TH17-modulating bile acid metabolites. *Nature* **603**, 907–912 (2022).
- 26. Hang, S. *et al.* Bile acid metabolites control TH17 and Treg cell differentiation. *Nature* **576**, 143–148 (2019).
- 27. Campbell, C. *et al.* Bacterial metabolism of bile acids promotes generation of peripheral regulatory T cells. *Nature* **581**, 475–479 (2020).
- 28. Song, X. *et al.* Microbial bile acid metabolites modulate gut RORγ+ regulatory T cell homeostasis. *Nature* **577**, 410–415 (2020).
- 29. Chung, H. *et al.* Gut Immune Maturation Depends on Colonization with a Host-Specific Microbiota. *Cell* **149**, 1578–1593 (2012).
- 30. Ansaldo, E., Farley, T. K. & Belkaid, Y. Control of Immunity by the Microbiota. *Annu. Rev. Immunol.* **39**, 449–479 (2021).

- 31. Ohnmacht Caspar *et al*. The microbiota regulates type 2 immunity through RORγt+ T cells. *Science* **349**, 989–993 (2015).
- 32. Blander, J. M. & Medzhitov, R. Toll-dependent selection of microbial antigens for presentation by dendritic cells. *Nature* **440**, 808–812 (2006).
- 33. Sefik Esen *et al.* Individual intestinal symbionts induce a distinct population of RORγ+ regulatory T cells. *Science* **349**, 993–997 (2015).
- 34. Lathrop, S. K. *et al.* Peripheral education of the immune system by colonic commensal microbiota. *Nature* **478**, 250–254 (2011).
- 35. Kokai-Kun, J. F. *et al.* Use of ribaxamase (SYN-004), a β-lactamase, to prevent Clostridium difficile infection in β-lactam-treated patients: a double-blind, phase 2b, randomised placebocontrolled trial. *Lancet Infect. Dis.* **19**, 487–496 (2019).
- 36. Hedberg, M., Lindqvist, L., Tunér, K. & Nord, C. E. Effect of beta-lactamase inhibitors on beta-lactamases from anaerobic bacteria. *Eur. J. Clin. Microbiol. Infect. Dis.* **11**, 1100–1104 (1992).
- 37. Cubillos-Ruiz, A. *et al.* An engineered live biotherapeutic for the prevention of antibiotic-induced dysbiosis. *Nat. Biomed. Eng.* **6**, 910–921 (2022).
- 38. Pamer, E. G. Resurrecting the intestinal microbiota to combat antibiotic-resistant pathogens. *Science* **352**, 535–538 (2016).
- 39. Kelsic, E. D., Zhao, J., Vetsigian, K. & Kishony, R. Counteraction of antibiotic production and degradation stabilizes microbial communities. *Nature* **521**, 516–519 (2015).
- 40. Bogatyrev, S. R., Rolando, J. C. & Ismagilov, R. F. Self-reinoculation with fecal flora changes microbiota density and composition leading to an altered bile-acid profile in the mouse small intestine. *Microbiome* **8**, 19 (2020).

- 41. Soave, O. & Brand, C. D. COPROPHAGY IN ANIMALS: A REVIEW. *Cornell Vet* 4, (1991).
- 42. Donaldson, G. P., Lee, S. M. & Mazmanian, S. K. Gut biogeography of the bacterial microbiota. *Nat. Rev. Microbiol.* **14**, 20–32 (2016).
- 43. Rooks, M. G. & Garrett, W. S. Gut microbiota, metabolites and host immunity. *Nat. Rev. Immunol.* **16**, 341–352 (2016).
- 44. McCarville, J. L., Chen, G. Y., Cuevas, V. D., Troha, K. & Ayres, J. S. Microbiota Metabolites in Health and Disease. *Annu. Rev. Immunol.* **38**, 147–170 (2020).
- 45. Dong, Q. *et al.* Protection against Clostridioides difficile disease by a naturally avirulent strain. *Cell Host Microbe* **33**, 59-70.e4 (2025).
- 46. Furusawa, Y. *et al.* Commensal microbe-derived butyrate induces the differentiation of colonic regulatory T cells. *Nature* **504**, 446–450 (2013).
- 47. Arpaia, N. *et al.* Metabolites produced by commensal bacteria promote peripheral regulatory T-cell generation. *Nature* **504**, 451–455 (2013).
- 48. Barnes, A. M. T. *et al.* Enterococcus faecalis readily colonizes the entire gastrointestinal tract and forms biofilms in a germ-free mouse model. *Virulence* **8**, 282–296 (2017).
- 49. Hirt, H. *et al.* Dynamics of plasmid-mediated niche invasion, immunity to invasion, and pheromone-inducible conjugation in the murine gastrointestinal tract. *Nat. Commun.* **13**, 1377 (2022).
- 50. Becattini, S., Taur, Y. & Pamer, E. G. Antibiotic-Induced Changes in the Intestinal Microbiota and Disease. *Trends Mol. Med.* **22**, 458–478 (2016).

- 51. Modi, S. R., Lee, H. H., Spina, C. S. & Collins, J. J. Antibiotic treatment expands the resistance reservoir and ecological network of the phage metagenome. *Nature* **499**, 219–222 (2013).
- 52. Kang, K. *et al.* Expansion and persistence of antibiotic-specific resistance genes following antibiotic treatment. *Gut Microbes* **13**, 1900995 (2021).
- 53. Yassour, M. *et al.* Natural history of the infant gut microbiome and impact of antibiotic treatment on bacterial strain diversity and stability. *Sci. Transl. Med.* **8**, (2016).
- 54. d'Humières, C. *et al.* Perturbation and resilience of the gut microbiome up to 3 months after β-lactams exposure in healthy volunteers suggest an important role of microbial β-lactamases. *Microbiome* **12**, 50 (2024).
- 55. Li, X. *et al.* Differential responses of the gut microbiome and resistome to antibiotic exposures in infants and adults. *Nat. Commun.* **14**, 8526 (2023).
- 56. Ivanov, I. I. *et al.* Induction of Intestinal Th17 Cells by Segmented Filamentous Bacteria. *Cell* **139**, 485–498 (2009).
- 57. Sommer, M. O. & Dantas, G. Antibiotics and the resistant microbiome. *Curr. Opin. Microbiol.* **14**, 556–563 (2011).
- 58. Huttenhower, C. *et al.* Structure, function and diversity of the healthy human microbiome. *Nature* **486**, 207–214 (2012).
- 59. Bush, K. & Bradford, P. A. Interplay between β-lactamases and new β-lactamase inhibitors.

 Nat. Rev. Microbiol. 17, 295–306 (2019).
- 60. Dugatkin, L. A., Perlin, M., Lucas, J. S. & Atlas, R. Group-beneficial traits, frequency-dependent selection and genotypic diversity: an antibiotic resistance paradigm. *Proc. R. Soc. B Biol. Sci.* **272**, 79–83 (2005).

- 61. Oliveira, R. A. & Pamer, E. G. Assembling symbiotic bacterial species into live therapeutic consortia that reconstitute microbiome functions. *Cell Host Microbe* **31**, 472–484 (2023).
- 62. Liu, Y. *et al.* Clostridium sporogenes uses reductive Stickland metabolism in the gut to generate ATP and produce circulating metabolites. *Nat. Microbiol.* **7**, 695–706 (2022).
- 63. Medaney, F., Dimitriu, T., Ellis, R. J. & Raymond, B. Live to cheat another day: bacterial dormancy facilitates the social exploitation of β-lactamases. *ISME J.* **10**, 778–787 (2016).
- 64. CLSI. Performance Standards for Antimicrobial Susceptibility Testing. *Clinical and Laboratory Standards Institute* **33rd ed.**, (2023).
- 65. Stiefel, U., Tima, M. A. & Nerandzic, M. M. Metallo-β-Lactamase-Producing Bacteroides Species Can Shield Other Members of the Gut Microbiota from Antibiotics. *Antimicrob*. *Agents Chemother*. **59**, 650–653 (2015).
- 66. Brook, I. The role of beta-lactamase-producing-bacteria in mixed infections. *BMC Infect. Dis.* **9**, 202 (2009).
- 67. Diebold, P. J. *et al.* Clinically relevant antibiotic resistance genes are linked to a limited set of taxa within gut microbiome worldwide. *Nat. Commun.* **14**, 7366 (2023).
- 68. Nord, C. E. Mechanisms of f3-Lactam Resistance in Anaerobic Bacteria.
- 69. Yeh, T.-K., Lin, H.-J., Liu, P.-Y., Wang, J.-H. & Hsueh, P.-R. Antibiotic resistance in Enterobacter hormaechei. *Int. J. Antimicrob. Agents* **60**, 106650 (2022).
- 70. Finegold, S. M. *et al.* Clostridium clostridioforme: a mixture of three clinically important species. *Eur. J. Clin. Microbiol. Infect. Dis.* **24**, 319–324 (2005).
- 71. Haas, K. N. & Blanchard, J. L. Reclassification of the Clostridium clostridioforme and Clostridium sphenoides clades as Enterocloster gen. nov. and Lacrimispora gen. nov., including reclassification of 15 taxa. *Int. J. Syst. Evol. Microbiol.* **70**, 23–34 (2020).

- 72. Dehoux, P. *et al.* Comparative genomics of Clostridium bolteae and Clostridium clostridioforme reveals species-specific genomic properties and numerous putative antibiotic resistance determinants. *BMC Genomics* 17, 819 (2016).
- 73. Garcillán-Barcia, M. P., Redondo-Salvo, S. & De La Cruz, F. Plasmid classifications. *Plasmid* **126**, 102684 (2023).
- 74. Grindley, N. D. F., Whiteson, K. L. & Rice, P. A. Mechanisms of Site-Specific Recombination. *Annu. Rev. Biochem.* **75**, 567–605 (2006).
- 75. Mazuet, C. *et al.* A penicillin- and metronidazole-resistant Clostridium botulinum strain responsible for an infant botulism case. *Clin. Microbiol. Infect.* **22**, 644.e7-644.e12 (2016).
- 76. Sorbara, M. T. *et al.* Functional and Genomic Variation between Human-Derived Isolates of Lachnospiraceae Reveals Inter- and Intra-Species Diversity. *Cell Host Microbe* **28**, 134-146.e4 (2020).
- 77. Philippon, A., Slama, P., Dény, P. & Labia, R. A Structure-Based Classification of Class A β-Lactamases, a Broadly Diverse Family of Enzymes. *Clin. Microbiol. Rev.* 29, 29–57 (2016).
- 78. Krogh, T. J., Agergaard, C. N., Møller-Jensen, J. & Justesen, U. S. Draft Genome Sequence of Parabacteroides goldsteinii with Putative Novel Metallo-β-Lactamases Isolated from a Blood Culture from a Human Patient. *Genome Announc*. **3**, e00937-15 (2015).
- 79. Zhang, Z. J. *et al.* Comprehensive analyses of a large human gut Bacteroidales culture collection reveal species- and strain-level diversity and evolution. *Cell Host Microbe* **32**, 1853-1867.e5 (2024).
- 80. Hu, J. *et al.* Molecular characteristics of global β-lactamase-producing Enterobacter cloacae by genomic analysis. *BMC Microbiol.* **22**, 255 (2022).

- 81. Becattini, S. *et al.* Rapid transcriptional and metabolic adaptation of intestinal microbes to host immune activation. *Cell Host Microbe* **29**, 378-393.e5 (2021).
- 82. Khan, A. A. *et al.* Polymorphic Immune Mechanisms Regulate Commensal Repertoire. *Cell Rep.* **29**, 541-550.e4 (2019).
- 83. Sóki, J., Keszőcze, A., Nagy, I., Burián, K. & Nagy, E. An update on ampicillin resistance and β-lactamase genes of Bacteroides spp. *J. Med. Microbiol.* **70**, (2021).
- 84. Worby, C. J. *et al.* Gut microbiome perturbation, antibiotic resistance, and Escherichia coli strain dynamics associated with international travel: a metagenomic analysis. *Lancet Microbe* **4**, e790–e799 (2023).
- 85. Bengtsson-Palme, J. *et al.* The Human Gut Microbiome as a Transporter of Antibiotic Resistance Genes between Continents. *Antimicrob. Agents Chemother.* **59**, 6551–6560 (2015).
- 86. Lee, K. *et al.* Population-level impacts of antibiotic usage on the human gut microbiome. *Nat. Commun.* **14**, 1191 (2023).
- 87. Darby, E. M. *et al.* Molecular mechanisms of antibiotic resistance revisited. *Nat. Rev. Microbiol.* **21**, 280–295 (2023).
- 88. Davin-Regli, A., Lavigne, J.-P. & Pagès, J.-M. *Enterobacter* spp.: Update on Taxonomy, Clinical Aspects, and Emerging Antimicrobial Resistance. *Clin. Microbiol. Rev.* **32**, e00002-19 (2019).
- 89. Queenan, A. M. & Bush, K. Carbapenemases: the Versatile β-Lactamases. *Clin. Microbiol. Rev.* **20**, 440–458 (2007).

- 90. Tshishonga, K. & Serepa-Dlamini, M. H. Draft Genome Sequence of Enterobacter hormaechei Strain MHSD6, a Plant Endophyte Isolated from Medicinal Plant *Pellaea calomelanos*. *Microbiol. Resour. Announc.* **8**, e01251-19 (2019).
- 91. Asimakis, E., Doudoumis, V., Gouvi, G. & Tsiamis, G. Draft Genome Sequence of Enterobacter hormaechei ENT5, a Component of the Symbiotic Community of Tephritid Flies. *Microbiol. Resour. Announc.* **8**, e01364-19 (2019).